Available online at www.sciencedirect.com
SCIENCE DIRECT®
Aquacultural Engineering 34 (2006) 275–302
aquacultural engineering
www.elsevier.com/locate/aqua-online

Design and management of conventional fluidized-sand biofilters

Steven T. Summerfelt *

The Conservation Fund Freshwater Institute, 1098 Turner Road, Shepherdstown, WV 25443, USA

Abstract

Fluidized-sand beds are an efficient, relatively compact, and cost-competitive technology for removing dissolved wastes from recirculating aquaculture systems, especially in relatively cool or coldwater applications that require maintaining consistently low levels of ammonia and nitrite. This paper describes several types of flow injection mechanisms used in commercial fluidized-sand biofilters and provides criteria for design of flow distribution mechanisms at the bottom of the fluidized bed. This paper also summarizes the most critical aspects of sand selection, as well as methods for calculating or experimentally measuring fluidization velocities and pressure drop for a given filter sand size distribution. Estimates of nitrification rate, ammonia removal efficiency, carbon dioxide production, and oxygen consumption across fluidized-sand biofilters are also provided for various conditions. Fluidized-sand biofilter operational and management practices are also described.

Keywords: Fluidize; Biofilter; Biofiltration; Ammonia removal; Sand; Water recirculation or reuse; Aquaculture

1. Introduction

Biofilter selection influences capital and operating costs of recirculating aquaculture systems, their water quality, and even the consistency of water treatment. A perfect biofilter would remove all of the ammonia entering the unit, produce no nitrite, support dense microbial growth on an inexpensive support material that does not capture solids, require little or no water pressure or maintenance, and require a small footprint. Unfortunately, no biofilter type can meet all of these objectives, but each biofilter type has there own advantages and limitations. In addition, different factors considered in biofilter selection can shift in relative importance depending upon production system requirements. For example, in recirculating systems used to culture salmonids, which are species that are relatively sensitive to unionized ammonia- and nitrite-nitrogen, a biofilter's capacity to reliably maintain low levels of total ammonia-nitrogen and nitrite-nitrogen could be as important a consideration

* Tel.: +1 304 870 2211; fax: +1 304 870 2208.
E-mail address: s.summerfelt@freshwaterinstitute.org.

0144-8609
doi:10.1016/j.aquaeng.2005.08.010

Nomenclature

A_b	cross-sectional area of fluidized bed column (cm^2)
A_{orif}	area of orifice (cm^2 or m^2)
A1	fluidization constant, $\frac{\varepsilon^3}{(1-\varepsilon)^2}\frac{\rho(\rho_p-\rho)g(\psi D_{eq})^3}{6^3\mu^2}$
C	orifice discharge coefficient for sharp-edged, submerged orifices (0.6)
D_{eq}	equivalent diameter, diameter of a sphere with the same volume as the particle of media (cm)
D_{10}	effective size, size of an opening which will pass only the smallest 10% of the granular media (cm)
D_{50}	mean size, sieve size which will pass 50% of the granular media (cm)
D_{60}	sieve size which will pass 60% of the granular media (cm)
D_{90}	calculating size, sieve size which will pass 90% of the granular media (cm)
g	gravity constant (980 cm/s^2)
H_{bed}	headloss due to flow through a granular bed (cm of water)
H_{orif}	headloss due to flow through orifice (cm of water)
L	depth of loosely-packed (static) granular-media bed (cm)
L_e	depth of expanded (fluidized) granular-media bed (cm)
ΔP	headloss across a bed of granular media, m of H_2O
Q_{biof}	flow rate of water through biofilter (L/min)
Q_{orif}	flow rate of water through orifice (cm^3/s)
Re_1	fluidization Reynolds number for expansion model, $\frac{\rho v_0 \psi D_{eq}}{6\mu(1-\varepsilon)}$
S_b	bed specific surface area (cm^{-1})
SG_p	specific gravity of the particle (unitless)
SG_w	specific gravity of water (1.0 unitless)
T	temperature (°C)
UC	uniformity coefficient
v_{mf}	minimum fluidization velocity (cm/s)
v_0	fluid superficial velocity (cm/s)
V_b	volume of bed (cm^3)

Greek letters

ε	static bed porosity of a loose packed bed, i.e., void fraction (unitless)
ε_e	expanded bed void fraction (unitless)
μ	fluid viscosity (g/cm/s)
ρ	fluid density (g/cm^3)
ρ_p	density of a particle of media (g/cm^3)
ψ	sphericity, the ratio of the surface area of a sphere of equal volume to the actual surface area of the particle (unitless)

as the biofilter's capital and operating costs (Summerfelt et al., 2001).

Conventional[1] fluidized-sand biofilters (FSBs) have been widely adopted in North America, especially in recirculating systems that must reliably maintain excellent water quality to produce species such as salmon smolt (Forsythe and Hosler, 2002; Holder, 2002; Wilton, 2002), arctic char (Summerfelt and Wade, 1998; Summerfelt et al., 2004a), rainbow trout (Heinen et al., 1996; Summerfelt et al., 2004b), endangered fish (Montagne, 2004), and tropical or ornamental fish (Weaver, 2005). FSBs can typically remove 50–90% of the ammonia each pass and thus maintain total ammonia-nitrogen and nitrite-nitrogen concentrations in their discharge of 0.1–0.5 mg/L and <0.1–0.3, respectively, in cold- and cool-water aquaculture systems (Heinen et al., 1996; Summerfelt et al., 2004b). FSBs can be less expensive and more compact than other biofilter types (Table 1), even when they are sized to provide excess nitrification capacity (Summerfelt and Wade, 1998; Timmons et al., 2000). The cost of surface area in FSBs is low (i.e., \$ 0.05–0.004 m^{-2} surface area) because filter sand has a high specific surface area (i.e., 4000–20,000 m^2/m^3) and is low cost, approximately \$ 70–200 m^{-3} of sand delivered (Summerfelt et al., 2004b). Individual FSBs can treat both small or large flows, with single FSBs treating as much as 190 L/s of water flow. FSBs can be circular or rectangular in shape, can

[1] Non-conventional fluidized biofilters use an expanded or moving bed media material other than sand, such as granular activated carbon, which is operated in an upflow configuration, or various types of relatively small plastic media, which are operated in either an upflow or a downflow configuration that depends upon the specific gravity of the media.

Table 1
Comparison of fixed costs associated with different biofilters that were all sized to meet the ammonia removal capacity for a tilapia farm capable of producing 454 Mton (1,000,000 lb) annually (from Timmons et al., 2000)

Biofilter type	Farm cost ($)	Cost, US$ per kg/year
Rotating biological contactor	668000	0.31
Trickling biofilter	620000	0.28
Bead filter	296000	0.14
Conventional fluidized-sand biofilter	124000	0.054
Cyclo biofilter	76000	0.036

be contained within plastic, fiberglass, concrete, or enamel-coated steel tanks, and can be constructed by personnel on site. In addition, FSBs can be relatively easy to manage because they do not filter solids from the passing flow and the actively growing microbial biomass in the expanded bed can be readily harvested by siphoning the lightest, i.e., thickest and oldest, biofilm coated particles from the top of the bed.

On the down-side, FSBs are relatively complex to design. FSB do not aerate, as do trickling filters. Therefore, FSBs should always be designed with a cascade column placed immediately downstream to strip dissolved carbon dioxide and bring the dissolved oxygen up to near 90% of saturation. FSB must also be operated within a fairly narrow water flow range, i.e., within about ±10–30% of its design flow, in order to maintain proper bed expansion. If water flow through a FSB ceases for more than approximately 6–24 h, depending upon conditions, the static but biologically active bed can turn anaerobic, resulting in a significant loss in nitrification capacity. Additionally, pumping water through a FSB requires water pressure to lift the sand bed (i.e., about 1.0 m of water head is required to expand every 1.0 m of static sand bed depth) and to overcome headloss designed into the FSBs flow inlet structure and any elevation difference between the water level in the pump sump and the top of the FSB (Summerfelt, 1996; Summerfelt et al., 2004b). Thus a total dynamic pumping head of 0.35–0.55 bar (5–8 psig), can be required to move water from the pump sump to the FSB overflow, depending largely upon the height of the FSB (Heinen et al., 1996; Summerfelt et al., 2004a, 2004b). In typical recirculating system designs for salmonid production (Summerfelt et al., 2004a, 2004b), once the water has been pumped through the FSB and exits the top of this vessel, the elevation achieved is used to gravity flow the water through the carbon dioxide stipping unit, low head oxygenator, culture tank, particle trap, and microscreen filter, returning to the pump sump. So the pumping energy through the FSB supplies approximately 90% of the mechanical power used within these recirculating systems, i.e., the remaining 10% of the mechanical power is used to ventilate the stripping columns and intermittently turn the drum filters.

The purpose of this paper is to provide design and operation criteria for conventional fluidized-sand biofilters. Toward this end the paper provides (1) methods and criteria for obtaining uniform flow distribution in FSBs, (2) criteria for filter sand selection, (3) techniques for measuring bed expansion for a given filter sand, (4) calculation of headloss across expanded beds, (5) calculations of the minimum water velocity required to provide fluidization and the bed expansion achieved at a given water velocity, (6) descriptions of the effects of biofilm growth on fluidization hydraulics and vertical stratification within the expanded bed, (7) estimates of nitrification rate and ammonia removal efficiency, (8) estimates of dissolved carbon dioxide production and dissolved oxygen consumption, and (9) practices for operating and managing FSBs.

2. Mechanisms for flow injection

Uniform water flow distribution at the base of the sand bed is critical for reliable operation of FSBs (Summerfelt and Cleasby, 1996; Summerfelt et al., 1996, 2004b). In addition to distributing an equal amount of flow across the base of the FSB, a properly designed flow distribution mechanism must also operate without detrimental fouling (or incorporate a mechanism to clear fouling from a plugged distribution system), prevent loss of filter sand, and support the sand bed in some designs. At least five different flow distribution mechanisms have been used to uniformly inject water at the base of large FSBs in recirculating aquaculture systems. Four of the five flow distribution mechanisms include a pipe manifold that originates at the top of the FSB and one or more vertical pipes that carry the flow down the inside of the

reactor to the base of the sand bed. Bringing flow into the FSB from above avoids having to penetrate the vessel's wall(s) with distribution pipes and also prevents the hydraulic head of water in the vessel from back flowing through the distribution piping when a siphon break or check valve has been installed.

The only flow distribution mechanism for FSBs that is commonly used in recirculating aquaculture systems that does not utilize a manifold at its top is the CycloBio® FSB, which is discussed in detail below. The CycloBio® FSB is also only supplied in a cylindrical vessel, whereas all of the other types of FSBs can be constructed with a cross-sectional area formed out of most any shape.

2.1. Gravel covered horizontal pipe or false floor manifold

One flow distribution system for FSBs consists of either a gravel covered pipe-manifold or false-floor distribution chamber that is sometimes used in relatively small recirculated systems (Malone and Burden, 1988) or in large-scale wastewater treatment systems (Jewell, 1990; Cooper and Atkinson, 1981; Sutton and Mishra, 1991). In some instances, one to four layers (each about 7.6 cm deep) of graded gravel are leveled over the distribution plate or piping, with the coarsest gravel next to the distribution plate or piping (Cleasby, 1990). However, high water velocities in the vicinity of the inlet orifices can cause gravel movement, particularly if the water velocity is not gradually increased during initial bed expansion (Cleasby, 1990). In addition, the gravel layers are not fluidized under normal operating conditions and, thus, are susceptible to plugging from solids entrapment and from microbiological growth. In order to avoid the use of layered gravel and its associated problems, industrial and municipal wastewater treatment applications have used nozzle-type flow distributors in combination with the false floor type flow distribution mechanism (Sutton and Mishra, 1991). However, when the distribution nozzle openings are small enough to exclude the majority of sand, there is an increased likelihood that the nozzles will plug or foul (Sutton and Mishra, 1991). In addition, their relatively high cost and proprietary nature has probably limited the application of more nozzle-type flow distribution systems that originated in the wastewater treatment industry.

2.2. Vertical pipe manifold

Possibly the first type of flow distribution mechanism developed specifically for application in recirculating aquaculture systems incorporates a pipe-manifold, originating at the top of the vessel, and then distributes the flow into vertical pipes that extend down to the base of the sand bed (Fig. 1) (Weaver, 1991, 2005). The vertical injection pipes are equally spaced across the plan area of the FSB and transport water flow to near the floor of the vessel where orifices in each probe uniformly distributes the flow directly into the sand (Fig. 1), without using layered gravel. If on occasion a flow injection probe plugs with sand, a mechanism is provided to flush the blockage from the probe. A fluidized-sand bed biofilter of this type, designed by Dr. Dallas Weaver (Scientific Hatcheries, Huntington Beach, CA), was used successfully at The Conservation Fund Freshwater Institute (Shepherdstown, WV) in the early 1990s (Heinen et al., 1996). This FSB design is marketed through Aquaneering Inc. (San Diego, CA) and has been widely applied in many types of recirculating aquaculture situations, but especially in applications that require fine sand FSBs to maintain high quality water (Weaver, 2005).

2.3. False floor orifice distribution plate

A second distribution mechanism specifically developed for application in recirculating aquaculture systems consists of a pipe manifold system that originates above the vessel and connects to a distribution chamber below a false-floor supporting the sand bed at the base of the vessel (Fig. 1). The central vertical pipe manifold is branched into four pipes, positioned in an H pattern when viewed from above, just before the four pipes connect to the false-floor. The false floor contains equally spaced orifices to uniformly distribute the water flow across the cross-sectional area at the base of the sand bed. The geometry of the distribution chamber, the location of the vertical laterals, and the spacing and size of the orifices are dependent upon the flow of water and on the diameter of sand (Eric Swanson, Maritime Aqua Service Ltd., Northeast Harbour, Maine, personal communication, 1993). A FSB of this type can be purchased from Legay Fiberglass Limited (Waverley, NS, Canada).

2.4. Horizontal pipe manifold

Another flow distribution mechanism, the horizontal pipe manifold system (Fig. 1), was also developed specifically for application in FSBs for recirculating aquaculture systems (Summerfelt, 1996; Summerfelt et al., 1996). Design of the horizontal pipe manifold flow distribution mechanism was based on the pipe lateral system used to backwash gravity sand filters that are typically found in municipal drinking

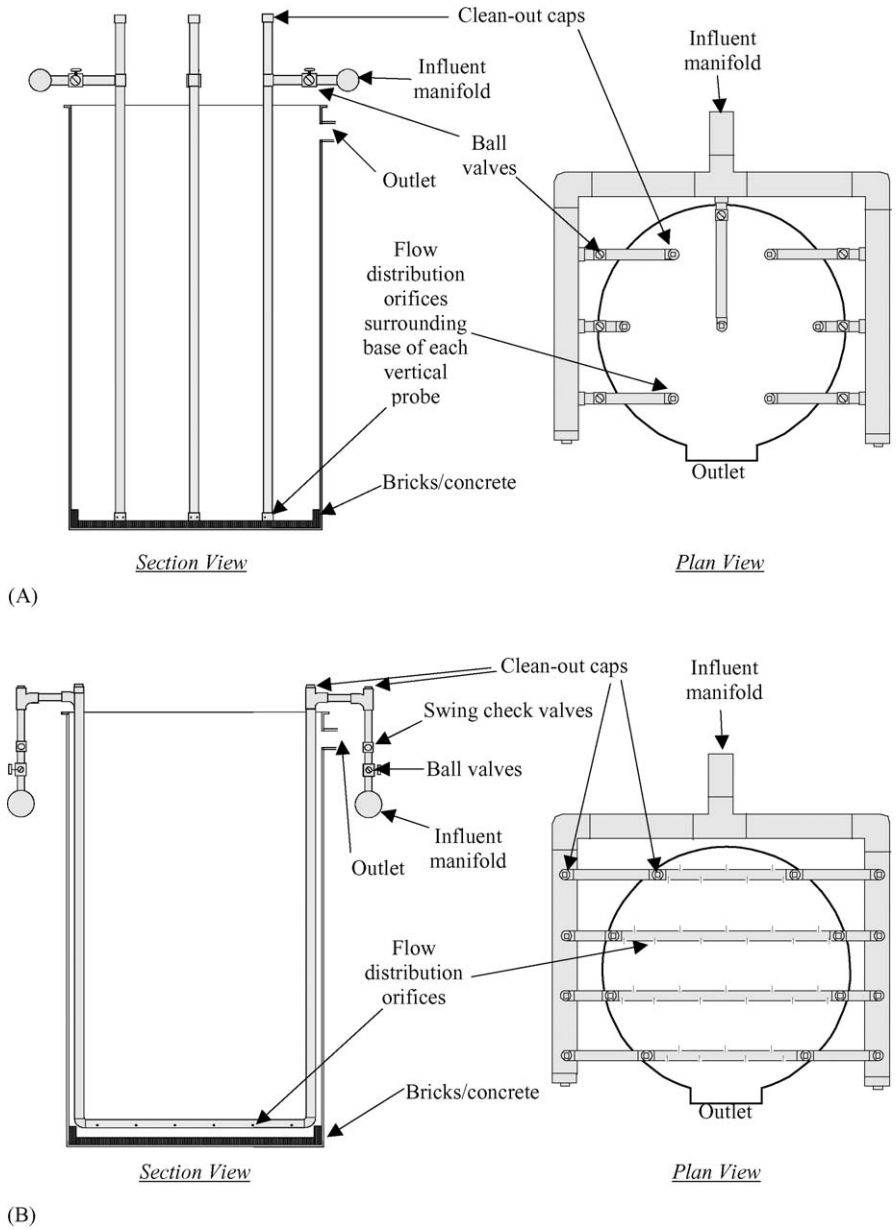

Fig. 1. Four of the most common flow distribution manifold systems used in conventional fluidized-sand biofilters for recirculating aquaculture systems include: (A) the vertical pipe manifold, (B) the horizontal pipe manifold, (C) the false floor orifice distribution plate, and (D) the CycloBio® w/slotted inlet manifold.

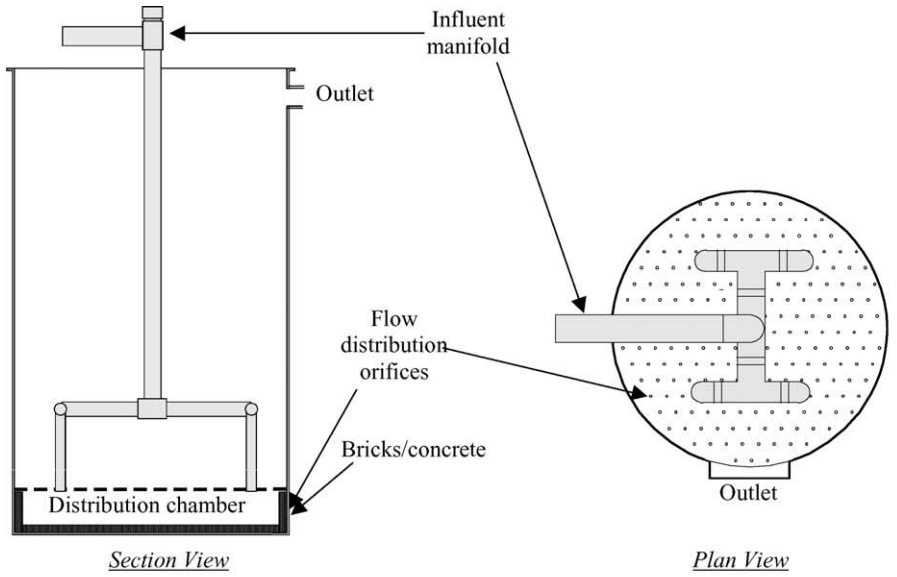

(C)

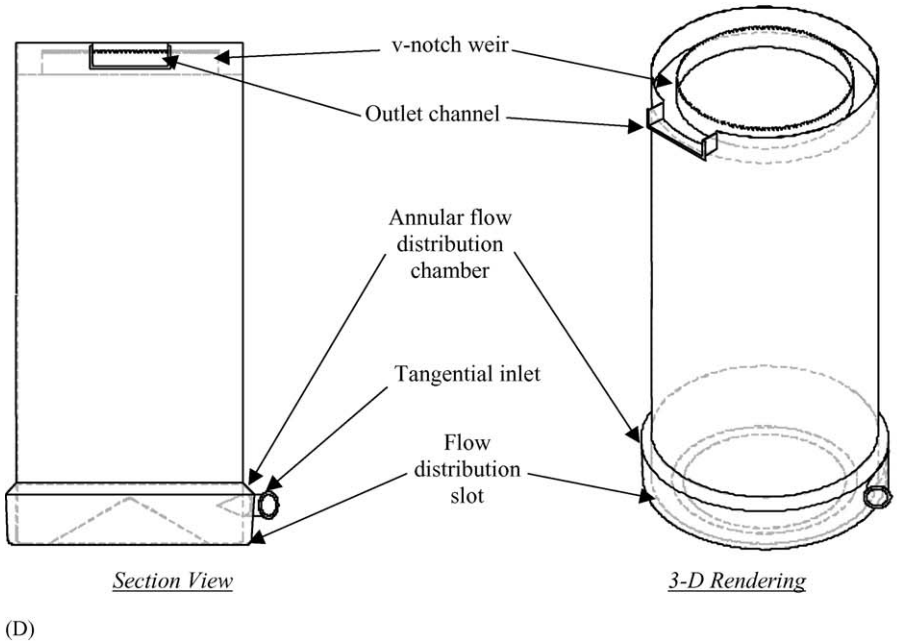

(D)

Fig. 1. (*Continued*).

water and wastewater applications. However, the flow distribution system was modified so that the manifold originated and terminated at the top of the biofilter. The overhead manifold pipes distribute the flow to equally spaced vertical pipes that run down the inside wall of the vessel to its base (Fig. 1). At the base of the vessel, each vertical pipe elbows 90° and runs horizontally across the floor to the opposite wall

where it again elbows 90° to run up the wall to the top of the vessel (Fig. 1). Flow distribution orifices are located on the section of horizontal pipe running along the floor of the vessel (Fig. 1). This design places threaded caps or valves at the top and end of each distribution pipe (Fig. 1), which can be temporarily opened as necessary to flush sand or debris from individual distribution pipes that have plugged (Summerfelt et al., 1996). If even more vigorous action was required to unplug a lateral, a garden hose or wire-rooter can be run down through the top of the tee fittings (the threaded cap covered opening) to flush debris. This design also allows for installation of control valves between the manifold pipe and individual distribution pipes (Fig. 1), which allows more flow to be forced through individual pipes to flush out sand or other debris when necessary. A swing-flex type check valve, which is located between the pumps and pipe manifold located above the biofilter vessel, prevents the hydraulic head of water in the vessel from back flowing through the distribution piping when pump pressure is lost and the expanded bed is defluidizing. Alternatively, a reissued US Patent by Goldman and Rosenau (2000) claims a method where at least one channel or reservoir of fluid is provided over at least a selected portion of the distribution network, with fluid from such column/reserve being released with a vacuum breaker in order to maintain flow and pressure in the distribution network as the media bed is defluidized.

The horizontal pipe lateral FSB design has been applied in numerous coldwater recirculating aquaculture system applications in North America (Summerfelt et al., 1996, 2004a; Summerfelt and Wade, 1998; Forsythe and Hosler, 2002; Holder, 2002) and has been marketed by PRAqua Technologies (Nanaimo, BC, Canada).

Criteria for calculating the size and separation of pipe laterals and flow injection orifices for the horizontal pipe lateral type flow injection mechanisms are well understood (Weber, 1972; Montgomery, 1985; AWWA, 1990; Summerfelt, 1996). Flow injection orifices and pipe laterals are typically separated at fixed intervals of between 7.5 and 30 cm (3–12 in.). The size and number of flow injection orifices are selected to provide a constant and controlling loss of head at each orifice to produce an equal flow through all orifices. Montgomery (1985) recommends sizing the distribution orifices to create an orifice headloss of at least 0.6 m. However, an orifice headloss of just greater than the headloss across the expanded bed can be expected to provide equal flow distribution, assuming that the distribution system is sized so that the flow velocity within the pipes are reasonably low and uniform throughout the filter area (Weber, 1972; Montgomery, 1985; AWWA, 1990). The headloss across an orifice of a given diameter at a given water flow rate can be estimated from the following equation:

$$H_{\text{orif}} = \left(\frac{Q_{\text{orif}}}{CA_{\text{orif}}}\right)^2 \frac{1}{2g} \quad (1)$$

where H_{orif} is the headloss due to flow through orifice (m of water); Q_{orif} the flow rate of water through orifice (m^3/s); A_{orif} the area of orifice (m^2); g the gravity constant (9.81 m/s^2); C the orifice discharge coefficient for sharp-edged, submerged orifices (0.6).

In practice, flow distribution orifices of approximately 6.4–12.7 mm (0.25–0.5 in.) diameter are recommended (Weber, 1972; Montgomery, 1985; AWWA, 1990). The flow distribution orifices should be aligned in two rows located on opposite sides of each horizontal pipe, running the length of the horizontal pipe, and "directed downward so as to dissipate the energy of the water jets" (Weber, 1972). Additional ratios are provided by Weber (1972) to act as guidelines to size the orifices, pipe laterals, and pipe manifold in order to obtain uniform flow distribution, i.e.,

$$\text{total area of orifices : cross-sectional area of bed} \cong 0.0015 \text{ to } 0.005 : 1 \quad (2)$$

$$\text{cross-sectional area of pipe-lateral : total area of orifices served} \cong 2 \text{ to } 4 : 1 \quad (3)$$

$$\text{cross-sectional area of manifold : total area of pipe-laterals served} \cong 1.5 \text{ to } 3 : 1 \quad (4)$$

Use of these ratios during the design of the flow distribution mechanism will help to (a) select pipe manifold and lateral sizes that produce water velocities that are reasonably low and uniform throughout the entire filter area, and (b) provide injection orifice

velocities suitable for introducing a controlling headloss (Montgomery, 1985). Creating a headloss across the orifice that is much lower than the head required to expand the sand bed would not provide uniform flow distribution under the sand bed, but rather it would produce water spouting through regions of the bed while other regions of the bed remain static. In contrast, an orifice headloss that is significantly larger than the head required to expand the sand bed would increase pumping costs and also produce a jetting action that would be more likely to damage the base of the vessel and abrade the sand in the jetting zone. Water jets emitting from the downward facing orifices (at an angle 45° below horizontal) have been known to sand blast holes through a 6 mm thick fiberglass floor of a FSB within only 7 days of start-up (Summerfelt et al., 1996). The AWWA (1971) has also reported on jet action producing problems at the base of filter beds. Therefore, to reduce the likelihood of the nozzle created jet action from ''sand-blasting'' through the vessel wall or floor, an abrasion resistant concrete pad or brick liner should be constructed on the biofilter floor, approximately 10–15 cm below the distribution pipes, and around the bottom 10–20 cm of the sides of the FRP vessel (Summerfelt et al., 1996).

2.5. *CycloBio® with slotted inlet manifold*

The CycloBio® FSB was developed by Neil Helwig of Marine Biotech Inc. (Beverly, MA) specifically for application in recirculating aquaculture systems, but it uses a flow distribution mechanism that is radically different from that used by the vertical pipe manifold, horizontal pipe-manifold, and false-floor flow distribution mechanisms (Fig. 1) (Timmons et al., 2000; Summerfelt et al., 2001, 2004b). The CycloBio® FSB injects water tangentially into an annular space that surrounds the base of the circular vessel and is integrated with the vessel wall. This continuous tangential injection of water through the annular space creates strong water rotation within the annular chamber and also forces water to enter the FSB vessel through a slot at the base of the sand bed and around the circumference of the vessel (Fig. 1). An inverted cone, incorporated into the center of the floor of the vessel (Fig. 1), is used to increase the upward-flowing water velocity at the base of the sand bed, which helps to improve sand bed expansion. Water flow injection within a CycloBio® FSB has some analogies with the slotted inlet design that is used to uniformly introduce air within agriculture livestock buildings (Timmons et al., 2000). However, the strong rotating flow created within the annular space of a CycloBio® FSB also imparts a cyclonic rotation within the expanded sand bed when clean sand bed expansion exceeds approximately 60–80%. The water velocity through the CycloBio® inlet slot is relatively small compared to the water velocity passing through the flow injection orifices on horizontal pipe lateral flow distribution mechanisms. Therefore, the CycloBio® FSB operates with relatively little headloss across the flow inlet slot (i.e., approximately 0.2–0.4 psig), which is approximately 1.5–2.0 psig less than the orifice headloss designed into horizontal pipe manifold flow distribution mechanisms (Summerfelt et al., 2004b).

Cyclonic rotation of the sand bed is a significant force contributing to uniform bed expansion in a CycloBio® FSB (Summerfelt et al., 2004b). In addition, CycloBio® FSBs appear to operate with more uniform bed expansion when their expanded bed depth is $\geq$ twice the diameter of the vessel (Summerfelt et al., 2004b). Under these conditions, CycloBio® FSBs have been found to be simple to operate and to re-fluidize after shut down (Summerfelt et al., 2004b). However, if a check valve failure or other unexpected event allows water to backflow through the CycloBio® vessel's tangential inlet, the plugged annular chamber that results can be rapidly cleared of packed sand by removing the blind flange covering an access port into the annular chamber and briefly turning on the pump supplying the FSB to flush sand from the inlet area. Experience at TCFFI has shown that when the blind flange has been reinstalled over the access cover, the CycloBio® FSB can re-fluidize and clear the remaining sand from the annular chamber. Note that the blind flange over the access port into the annular chamber must not be removed until after water inside the vessel has been removed. In addition, no floor abrasion below the slotted inlet has been observed in the two large-scale CycloBio® FSBs evaluated at TCFFI, probably because the water velocities at the inlet slot are relatively low and the water is injected parallel to the vessel floor (Summerfelt et al., 2004b).

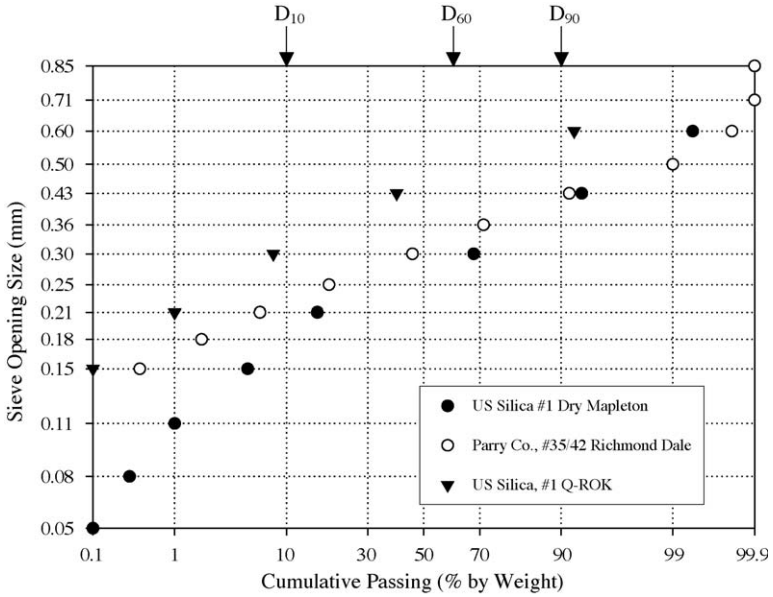

Fig. 2. Sieve analysis of three filter sands that were evaluated in fluidized-sand biofilters at the Conservation Fund Freshwater Institute. The sand's D_{10}, D_{60}, and D_{90} are the sieve opening sizes that would pass only the smallest 10, 60, or 90% of the granular sample by weight. D_{10} is the sand's effective size.

CycloBio® FSBs can be purchased from Marine Biotech Inc.

All of the flow distribution mechanisms described above, except those mechanisms that rely on layered gravel or inlet nozzle structures, have typically worked well in FSBs used in recirculating aquaculture systems. However, as in the wastewater treatment industry (Sutton and Mishra, 1991), the gravel-covered and nozzle structure covered distribution systems have had some problems with plugging and channeling in large filters.

3. Sand selection criteria

FSBs use extremely hard, whole grain, finely graded crystalline silica sand, which has a specific gravity of 2.65. Silica filter sand suppliers can be located by searching the World Wide Web or a list of filter sand suppliers such as is provided by AWWA (2004). Filter sands are typically pre-sieved to produce a distinct size range, which is usually specified by an effective size and uniformity coefficient (Cleasby, 1990). ASTM (1985) standard test procedure C136-84a should be used for conducting sieve analysis of a granular sample. The sand's effective size (D_{10}) is the sieve opening size that would pass only the smallest 10% of the granular sample by weight, as read from the log-probability plot of the sieve analysis for a given sand sample (Fig. 2). The sand's uniformity coefficient (UC) is a quantitative measure of the variation in particle size within the sand sample that is defined as the ratio of D_{60}:D_{10}. The sand's D_{60} is the size for which 60% of the sand is smaller by weight, as read from the same log-probability plot of the sieve analysis results (Fig. 2).

The D_{10} is the fraction of sand that will expand[2] the most at a given superficial velocity in a FSB. The D_{90}, an estimate of the sand diameter of the largest 10% of sand in the sample, is the sand fraction that will expand the least at a given superficial velocity. The D_{90} can also be read from the log-probability plot of

[2] When a sand bed is expanded, its total height is some percentage greater than its initial static height. Percent bed expansion is calculated by subtracting the expanded bed height from the static bed height, dividing this difference by the static bed height, and then multiplying by 100.

the sieve analysis for the sand in question (Fig. 2). Alternatively, the D_{90} can be estimated if the D_{10} and UC of the sand are supplied with the use of the following equation (Cleasby, 1990):

$$D_{90} = D_{10} \times 10^{1.67 \log(\mathrm{UC})} \quad (5)$$

The size and UC of filter sand are both critical for successful application in FSBs. Sand grains with relatively larger diameters will generally migrate towards the bottom of a FSB where they expand less than the relatively smaller sands that have migrated to the top of the bed. For a given graded sand placed in a FSB, the D_{90} fraction of the sand must expand at least 10–20% at the design superficial velocity in order to minimize occurrence of static sand piles at the base of the bed. At the same time, the D_{10} fraction of sand must not expand excessively (e.g., over 150–200%) to prevent it from washing out the top of the FSB (Summerfelt and Cleasby, 1996).

Sands used in FSBs for recirculating aquaculture systems may have a D_{10} as small as 0.1 mm or as large as 1.0 mm, as well as a uniformity coefficient ranging from 1.3 to 1.8. A smaller UC is more ideal for filter sands, as this represents a smaller variation in the sand size distribution. During FSB design, a filter sand is selected that will provide a given D_{10} and size distribution that produces a mean clean-sand bed expansions of typically between 40 and 100% at a given superficial water velocity (Summerfelt and Cleasby, 1996). Final expansion of a FSB established with biofilm may reach 200–300%. Unfortunately, proper filter sand selection can be somewhat challenging. For this reason, during FSB design the sand bed expansion for a given sand source should be estimated at various superficial water velocities using both experimental test column studies and empirical calculations based upon the sand's D_{10}, D_{50}, and D_{90}.

3.1. Calculating pressure drop

Water injected into the base of a FSB will flow up through void spaces between sand granules in the initially static bed. Water flowing through the sand bed must overcome both viscous and inertial forces (Ergun, 1952), which combine to create an overall pressure drop across the static bed that increases with increasing water flow (Fig. 3). The sand bed begins to

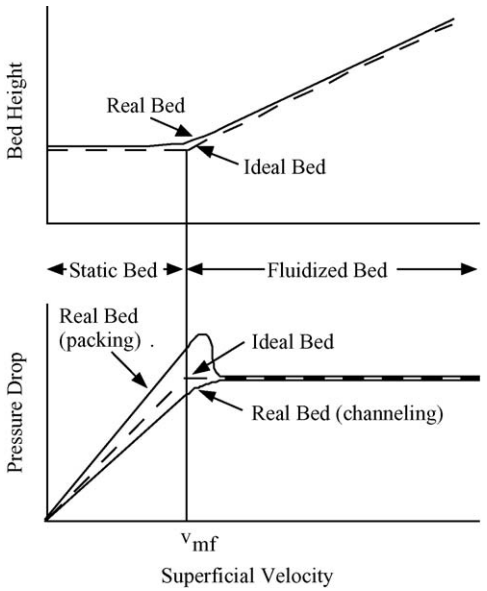

Fig. 3. Illustration of the hydraulics of flow through a bed of granular media at superficial velocities (Q/A_b) above and below the minimum fluidization velocity (v_{mf}) (as shown by Fan, 1981). The v_{mf} is the superficial velocity at the point of incipient fluidization.

expand when the water velocity through the sand void spaces is sufficient to create a pressure loss that is greater than the apparent weight (actual weight less buoyancy) per unit cross-sectional area of the bed (Denn, 1980; Cleasby, 1990). When the bed is fluidized, the individual sand granules are freely supported and tumble with the flow of water. The relative amount of sand bed expansion is dependent upon the density, shape and diameter of the particles, and the velocity of water (as discussed in the next section). Once the bed has been fluidized, the pressure drop across the bed remains constant at all bed expansions at up to about 90% porosity (Cleasby, 1990), as diagramed in Fig. 3.

When a sand bed is expanded, the net gravitational and buoyant force acting on the sand bed, i.e., the mass of the sand granules ($\rho_p g V_b\{1-\varepsilon\}$) minus the mass of the liquid that they displace ($\rho g V_b\{1-\varepsilon\}$), is equal to the net upward force on the bed ($\Delta P A_b$), where $(1-\varepsilon)$ is the fraction of bed volume occupied by sand granules ≅0.53–0.58 (unitless), ε the void fraction (i.e., porosity) of the loose static bed ≅0.42–0.47 (unitless), ρ the density of water (1.0 g/cm^3), ρ_p the density of sand (2.65 g/cm^3), g the force of gravity (980 cm/s^2); A_b the cross-sectional area of the bed in

cm^2; V_b the volume of the bed in cm^3, and ΔP the pressure drop across the fluidized bed in dyne/cm^2.

Recognizing that the ΔP across the fluidized bed is equal to the product of the headloss across the bed (H_{bed}, in cm of water), g, and ρ, then simplifying the force balance will produce the constant headloss equation for expanded beds (Denn, 1980):

$$\frac{H_{bed}}{L} = \frac{\rho_p - \rho}{\rho}(1-\varepsilon) = (SG_p - SG_w)(1-\varepsilon) \quad (6)$$

where L is the depth of the static bed in cm, SG_p the specific gravity of the particle (unitless), and SG_w is the specific gravity of water (unitless).

This equation can be used to calculate the headloss per unit static bed depth, i.e., h/L, for an expanded bed of granular particles. Based upon this equation, a fluidized bed of sand would require approximately 0.87–0.98 m of water head for every 1.0 m of initially static sand depth, if a static bed porosity of 0.42–0.47 is assumed (Summerfelt and Cleasby, 1996). Note from Eq. (6) that the headloss across an expanded bed is independent of sand size.

3.2. Calculating bed expansion as a function of water velocity and sand size

Expansion of a clean sand bed can be estimated for a given superficial water velocity if the sand's diameter, UC, ρ_p, ε, and sphericity (ψ) are known as well as the fluid's ρ and viscosity (μ), both of which are temperature dependent (Wen and Yu, 1966; Dharmarajah and Cleasby, 1986). As described in Table 2, these sand characteristics can be determined from preliminary laboratory fluidization studies and sieve analyses on samples of the same sand. These studies require facilities and time, not only to perform the studies but also to obtain the sand samples. Alternatively, the ρ_p, ε, and ψ of many sand sources can typically be assumed to be within the range of 2.645–2.655, 0.42–0.47, and 0.7–0.8, respectively (Cleasby, 1990), for a loosely packed sand. The D_{10}, D_{50}, D_{90}, and UC of each filter sand supply must still be determined from a sieve analysis (Fig. 2), but the sieve analysis can be obtained from the supplier. After the D_{10}, D_{50}, D_{90}, UC, ρ_p, ε, and ψ for a given sand are obtained or assumed, these values can be used to calculate the superficial water velocity required to achieve a given bed expansion at a given water temperature, as will be discussed below.

3.2.1. Minimum fluidization velocity

Wen and Yu (1966) developed an equation to predict the minimum fluidization velocity (v_{mf}) at the point of incipient fluidization of the sand, which only requires knowledge of the equivalent diameter of the sand granule (D_{eq}), ρ_p, ρ and fluid viscosity (μ):

$$v_{mf} \cong \frac{\mu}{\rho D_{eq}}\left(33.7^2 + 0.0408 D_{eq}^3 \frac{\rho(\rho_p - \rho)g}{\mu^2}\right)^{0.5} - \frac{33.7\mu}{\rho D_{eq}} \quad (7)$$

3.2.2. Bed expansion versus velocity

The porosity of an expanded bed (ε_e), which can never exceed 1.0 as the expanded bed depth goes to infinity, can be calculated from ε, L, and the expanded bed depth (L_e), e.g. (Weber, 1972):

$$\varepsilon_e = 1 - (1-\varepsilon)\frac{L}{L_e} \quad (8)$$

The ε_e can also be predicted for a given superficial velocity (v_0) and a given sand D_{eq}, ρ_p, ψ and ε, as well as the water's ρ and μ using a phenomenological model developed by Dharmarajah and Cleasby (1986). The model of Dharmarajah and Cleasby (1986) results in a plot of two dimensionless numbers, A1 and Re_1:

$$A1 = \frac{\varepsilon^3}{(1-\varepsilon)^2}\frac{\rho(\rho_p - \rho)g(\psi D_{eq})^3}{6^3\mu^2},$$
$$Re_1 = \frac{\rho v_0 \psi D_{eq}}{6\mu(1-\varepsilon)} \quad (9)$$

Dharmarajah and Cleasby (1986) fit the curve resulting from the plot of A1 versus Re_1 using a step-wise regression procedure, and report the polynomial relationship:

$$\log(A1) \cong \begin{cases} 0.56543 + 1.09348\log(Re_1) + 0.17971(\log(Re_1))^2 \\ -0.00392(\log(Re_1))^4 - 1.5(\log(\psi))^2 \end{cases} \quad (10)$$

Table 2
Calculations of media characteristics (from Summerfelt and Cleasby, 1996)

Property	Definition and method of determination
Static bed porosity, ε	*Definition*. The porosity of a static bed of granular media is the fraction of the volume within the bed which is not occupied by particles: $\varepsilon = \frac{\text{volume of voids}}{\text{volume of bed}}$. The porosity required for fluidization calculations is the porosity of the static bed after it has been fully expanded (200%) and has just been brought to rest by gradually cutting back the hydraulic loading rate until the flow is zero *Determination*. The static bed void fraction of the sample of clean sand can be calculated from the total mass of the clean sand sample, the total volume of the sand sample, and the density of sand: $\varepsilon = 1 - \left(\frac{(\text{total mass of sand})/(\text{particle density of sand})}{\text{volume of bed}}\right)$
Particle density, ρ_p	*Definition*. The density of a particle is the ratio of particle mass to particle volume including its pore volume but excluding inter-particle voids *Determination*. The density of a particle can be determined for porous and non-porous media *Non-porous media*: The density of non-porous media can be estimated by quantifying the volume displaced by a given mass of particles *Porous media*: Geldart (1990) described methods for calculating the density of porous particles
Bulk density of the bed, ρ_b	*Definition*. The density of the bed is ratio of bed mass (dry) to bed volume *Determination*. The density of the bed of granular media can be found by measuring the mass of the media and dividing by the volume that mass occupies
Particle size distribution	*Definition*. The particle size distribution is defined as the relative percentage by weight of grains of each the different size fractions represented in the sample *Determination*. The size distribution of a sample of sand is generally determined from a sieve analysis and results in a table of the percentage of media finer than a given opening size. A plot on log-probability graph paper of the "percent finer" (normal scale) vs. the corresponding sieve size (log scale) will show a straight line for most natural sands (Weber, 1972)
Effective size, D_{10}	*Definition*. The effective size is defined as the opening size that will pass only the smallest 10%, by weight, of the granular sample *Determination*. The D_{10} can be taken from a log-probability plot of the particle size distribution
Calculating size, D_{90}	*Definition*. The "calculating size" is the sieve size for which 90% of the grains by weight are smaller. The D_{90} provides an estimate of the largest sand in the sample and is the value used during design to calculate the velocity required to fluidize even the largest sand *Determination*. The D_{90} can be determined from the particle size distribution as plotted on log-probability paper or can be approximated (Cleasby, 1990) by: $D_{90} = D_{10} \times 10^{1.67\log(\text{UC})}$
Uniformity coefficient, UC	*Definition*. The uniformity coefficient is a quantitative measure of the variation in particle size of a given media and is defined as the ratio of D_{60}:D_{10} *Determination*. The UC for a given granular media equals the D_{60} divided by the D_{10} values which are determined after plotting the results of a sieve analysis on log-probability paper
Equivalent diameter, D_{eq}	*Definition*. The equivalent diameter of an irregular particle is defined as the diameter of a sphere with the same volume as the particle *Determination*. The average equivalent diameter of a sample of sand can be found by determining the mass of the average grain. The equivalent diameter of the sand can be calculated from: $D_{eq} = \left(\frac{6}{\pi}\frac{\text{average mass of one grain}}{\text{particle density of sand}}\right)^{1/3}$
Particle specific surface area, S_p	*Definition*. The particle specific surface area is defined as the surface area per unit of particle volume. The S_p for particles which are perfectly spherical can be calculated from: $S_p\,(\text{sphere}) = \frac{\text{sphere surface area}}{\text{sphere volume}} = \frac{4\pi R^2}{(4/3)\pi R^3} = \frac{3}{R} = \frac{6}{D}$ (where R and D are the radius and diameter of the sphere, respectively). The S_p for particles which are not completely uniform must take into account the particle's shape (e.g. sphericity, ψ, defined below): $S_p = \frac{\text{particle surface area}}{\text{particle volume}} = \frac{6}{\psi D_{eq}}$

Table 2 (*Continued*)

Property	Definition and method of determination
	Determination. If ψ is known, or can be assumed, then S_p can be calculated from D_{eq} and ψ using the equation directly above. If ψ is not simply assumed, the S_p can be determined from experiments measuring the headloss vs. flow rate across a loosely packed bed of granular media. A relationship between headloss and flow rate, developed by Ergun (1952), can be used for plotting granular media headloss data and solving for S_p according to the slope of the resulting line
Bed specific surface area, S_b	*Definition*. The bed specific surface area is the total surface area of particles per unit of bed volume *Determination*. The S_b is dependent upon how tightly the bed is packed or conversely on how much the bed is expanded. The S_b can be calculated for a given ε once S_p is known, e.g.: $S_b = S_p(1 - \varepsilon)$

These equations can be solved to accurately predict ε_e for a given v_0 and specific sand characteristics (Dharmarajah and Cleasby, 1986). However, the solution required to estimate ε_e is iterative.

Summerfelt and Cleasby (1996) have applied the Dharmarajah and Cleasby (1986) model to graphically relate the v_0 required to achieve bed expansions of 0, 50, 100, and 150% for sand D_{eq} sizes that range from 0.05 to 1.5 mm in freshwater, i.e., 0 ppt salinity, at 25 °C (Fig. 4). Note that the v_0 required to achieve a given ε_e for a given D_{eq} also depends upon the water's ρ and μ, which are both dependent upon the temperature and salinity of the water. For a given sand at a given v_0, sand bed expansion decreases with increasing temperature (Fig. 5), largely due to the corresponding decrease in μ. A large change in water temperature appears to create a larger affect on bed expansion than will a change from freshwater to nearly full-strength seawater (Fig. 5). Changing from freshwater (i.e., 0 ppt salinity) to seawater (i.e., 32 ppt salinity) will only cause a slight increase in overall sand bed expansion for a given D_{eq} at a given water temperature (Fig. 5).

Fig. 4 can be used to roughly estimate the expansion of the D_{10}, D_{50}, and D_{90} size classes for

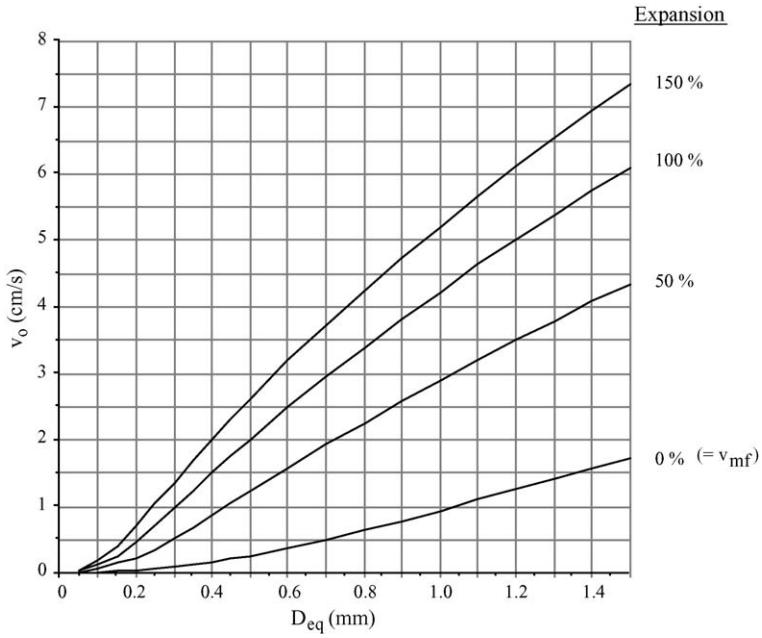

Fig. 4. Relationship between fluid superficial velocity (v_0) and bed expansion for sand of a uniform size (D_{eq}) assuming typical values for ψ (0.75), ε (0.45) and T (25 °C) (from Summerfelt and Cleasby, 1996).

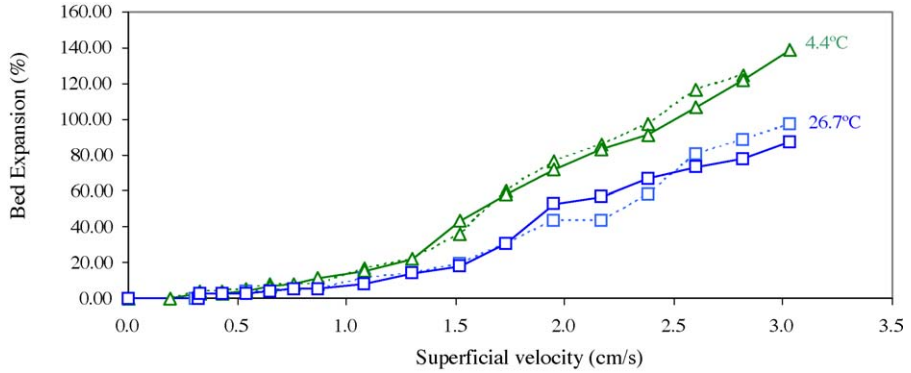

Fig. 5. Relationship between bed expansion and superficial velocity measured at water temperatures of 4.4 °C (△) and 26.7 °C (□) and at water salinities of 0 ppt (—) and 32 ppt (- - -) for a 20/40 sand expanded in a 0.61 m diameter CycloBio® containing 0.91 m depth of initially loose static sand. Data courtesy of Thomas Lauttenbach, Marine Biotech Inc., Beverly, MA.

a given filter sand at a given v_0. The bed expansion at a given v_0 should be calculated for each D_{10}, D_{50}, and D_{90} size classes of a specific filter sand, because the larger diameter sand fractions move to the bottom of a FSB where they are expanded to a much lower extent than the smaller sand fractions that have migrated to the top of the bed. For example, according to the sieve analysis reported in Fig. 2, the US Silica #1 Dry Mapleton sand has a D_{10}, D_{50}, and D_{90} of approximately 0.19, 0.28, and 0.40 mm, respectively, and these sand fractions would expand approximately 150, 80, and 35%, respectively, at a v_0 of 0.75 cm/s according to the bed expansion estimates provided in Fig. 4. In this example, it appears that the largest 10% of the sand would be expected to expand, whereas the finest 10–20% of the sand could be siphoned out of the FSB immediately after its initial bed expansion to reduce its likelihood of washing out when the biofilm becomes established. If the finest 10–20% of the sand was not removed, then the overall bed expansion of the US Silica #1 Dry Mapleton sand would be expected to be approximately 80% (i.e., the bed expansion at D_{50} = 0.28 mm), which is in approximate agreement with data collected from 10 cm diameter test column studies conducted at TCFFI (Summerfelt, unpublished data).

3.3. Experimental technique to measure bed expansion from a sample of filter sand

The author recommends that after the v_0 and ε_e have been estimated for a given filter sand, but before the recirculating aquaculture system design has been completed, that a sample of the specific filter sand under consideration be obtained and tested hydraulically to develop the most accurate estimate of the actual relationship between v_0 and ε_e.

In order to conduct bed expansion tests, order at least 8–14 L (0.3–0.5 ft^3) of a representative sample of the filter sand from the desired supplier. This sample will mass approximately 12–21 kg, because filter sand has a bulk density of approximately 1600 kg/m^3 (100 lb/ft^3). Fabricate a test column set-up that consists of a 10 cm nominal inside diameter clear PVC pipe with an overall height of approximately 2.7 m (9 ft). The test column should contain a 2.5 cm (1 in.) diameter inlet pipe located at the bottom end of the test column and a 2.5 cm (1 in.) diameter outlet pipe that is located within 30 cm (1 ft) of the column's open top. At the base of the column, the inlet pipe should be covered with at least 30 cm (1 ft) of layered gravel to distribute the flow under the sand for the short duration of the expansion test. A pressurized water line with a throttling valve that can supply anywhere from 0 to 16 L/min of water should be connected to the inlet pipe of the test column. A check valve should be located on the inlet water supply pipe, just before the supply pipe enters the test column, in order to prevent water from back flowing out the bottom of the test column. The outlet pipe near the top of the test column should be plumbed to discharge to a drain, but should also allow for bucket testing of the discharge flow rate. Approximately 1 m of sand

should be added to the test column. Sand should be poured into the top of the test column after the test column contains at least 1 m of water. Before the sand bed expansion tests begin, slowly open the throttling valve on the water supply until the sand bed in the test column has expanded approximately 0.6 m. Allow the test column to flush out fine particles for approximately 10–30 min. At this time, the top 10–20% of the expanded bed could be siphoned out if this will be the normal start-up procedure for the full-scale FSB. The depth of sand siphoned from the top of the expanded bed will depend largely upon the uniformity coefficient of the sand; siphoning is not required when the sand's UC approaches 1.3. The water flowing through the test column should be turned off slowly and the sand bed should be allowed to settle for a period of 30 min before the total depth of the loose packed static sand bed is measured. During this period of bed collapse, do not tap or vibrate the column to obtain more compression of the static sand. After recording the loose packed static bed depth, slowly turn up the water flow rate through the bed until the bed expands approximately 20% and then record the overall bed height at the corresponding water flow rate that has been determined using a bucket test or a calibrated flow meter. Repeat this test while increasing the water flow rates to increase the bed expansion in increments of approximately 20% (e.g., 20, 40, 60, 80, 100, and 120% bed expansions) until overall bed expansion equals or exceeds 120%. At this point all of the experimental data will be collected and the test column can be cleaned out and prepared for the next sand trial. The superficial water velocity (v_0) encountered during each of the test conditions can now be calculated from each of the water flow rates recorded (Q_{biof}, L/min), i.e., by dividing each flow rate by the cross-sectional area (A_b) of the column:

$$v_0 = \frac{Q_{biof}\,(\mathrm{L/min})}{A_b\,(\mathrm{cm^2})} \frac{1000\,(\mathrm{cm^3})}{1\,(\mathrm{L})} \frac{1\,(\mathrm{min})}{60\,(\mathrm{s})} \qquad (11)$$

The v_0 measured in test columns at sand bed expansions of 20, 50, 100, and 150% are reported in Table 3 for four filter sand samples with a D_{10} of approximately 0.24, 0.45, 0.60, and 0.80 mm. Table 3 also contains estimates of v_0 that were calculated using the Dharmarajah and Cleasby (1986) model, i.e., Eqs. (9) and (10), assuming ε and ψ of 0.45 and 0.75, respectively, a water temperature of 25 °C, and D_{50} for each sand of 0.37, 0.59, 0.79, and 0.99 mm. Comparing the two v_0 reported in Table 3, for a given sand at a given sand bed expansion, indicates that the Dharmarajah and Cleasby (1986) model can be used to estimate sand bed expansion. However, the assumption that each of the sand samples was represented by a ε and ψ of 0.45 and 0.75, respectively, and a D_{50} did create some error in estimating the v_0 requirements for a given sand (Table 3). Therefore, conducting the sand bed expansion tests in a test column is still deemed necessary.

Table 3
Water velocities required to expand four different sands approximately 20, 50, 100, and 150%

	Sands tested			
Retaining sieve mesh sizes	40/70	30/50	20/40	18/30
Effective size, D_{10} (mm)	0.24	0.45	0.60	0.80
Uniformity coefficient	1.8	1.4	1.4	1.3
D_{50} (mm)	0.37	0.59	0.79	0.99
Velocity requirements (cm/s)				
20% expansion	0.5/0.4	0.7/0.9	0.8/1.4	1.3/1.9
50% expansion	1.0/0.8	1.3/1.5	1.9/2.2	2.7/2.9
100% expansion	1.4/1.4	2.0/2.4	3.1/3.3	4.6/4.2
150% expansion	1.9/1.9	2.7/3.1	4.1/4.2	5.9/5.2

The four sands tested had a D_{10} of 0.24, 0.45, 0.60, and 0.80 mm. The first v_0 reported is an average of measurements made during fluidization tests in a 10 cm diameter test column. The second v_0 was predicted for the mean sand size (D_{50}) using the Dharmarajah and Cleasby (1986) model, assuming that ε and ψ are 0.45 and 0.75, respectively, and a water temperature of 25 °C.

3.4. Comparing sand bed expansion measured in test columns with full-scale FSB tests

Over the last decade, three of the five flow distribution mechanisms illustrated in Fig. 1 were evaluated at TCFFI in Shepherdstown, West Virginia, i.e., the vertical probe system (Heinen et al., 1996; Weaver, 2005), the horizontal pipe manifold (Summerfelt et al., 1996), and the CycloBio® FSB (Summerfelt et al., 2004b). The full-scale vertical probe FSB and the horizontal pipe manifold FSB both appeared to produce a sand bed expansion that were consistent with or slightly lower (within approximately

10%) than would be predicted by the expansion test column results. The slightly lower bed expansions that resulted could be explained by the occurrence of small sand mounds about the perimeter of the bed, which stored a small volume of sand that was not fluidized. However, when sand bed expansion within full-scale (2.7 m diameter) CycloBio® FSBs was compared with sand expansion tests that had been conducted within a 10 cm test column (Fig. 6), results indicate that a given sand expands roughly 10–40% less in a full-scale CycloBio® vessel than the same sand was found to expand in a 10 cm diameter test column for a given hydraulic loading rate (Summerfelt et al., 2004b). The finest sand tested, the #1 Mapleton sand (D_{10} = 0.18 mm) from US Silica, had the closest match for bed expansion when comparing the test column to the full-scale CycloBio® data. The consistently lower bed expansion in the full-scale CycloBio® FSB was probably due to water spouting along the wall of the vessel and to increased formation of transient sand mounds that were most prevalent when overall bed expansion was less than approximately 50% (Summerfelt et al., 2004b). Overall sand bed expansion within the full-scale CycloBio® FSB was closest to the sand bed expansion within the 10 cm diameter test column when overall bed expansion exceeded approximately 60% (Fig. 6). Because of these findings, during the design of a full-scale CycloBio® FSB, a given filter sand should be expected to expand approximately 10–40% less than was predicted during its test column evaluation.

3.5. Effect of biofilm growth on fluidization

Microorganisms that metabolize ammonia and other dissolved wastes grow as a biofilm attached to the sand surfaces and this attachment prevents the microorganims from being flushed out of the FSB (Cooper and Atkinson, 1981; Shieh et al., 1981; Chang et al., 1991; Summerfelt and Cleasby, 1996; Nam et al., 2000). Cooper and Atkinson (1981), Shieh et al. (1981), and Chang et al. (1991) have modeled biofilm growth and substrate uptake in detail. Biofilm thickness depends upon a complicated balance between two competing mechanisms: (1) growth rate of the biofilm and (2) physical shearing of the biofilm (Chang et al., 1991). Growth rate of the biofilm depends upon the makeup and age of the microorganism, as well as the type, concentration, and loading of the growth limiting substrate. The physical shearing of the biofilm depends upon the intensity of fluid shear, particle–particle collisions, and particle–wall collisions (Chang et al., 1991). The process is complicated because of the interdependence of the biofilm growth and shearing mechanisms.

Biofilm growth increases the volume occupied by particles and decreases the effective density of the biofilm coated sand, which in turn increases the bed volume and overall expansion of these particles. Increased expansion due to biofilm growth can be of special significance when fine sand (D_{10} = 0.15–0.3 mm) is used within the FSB, as the biofilm thickness may become greater than the diameter of the sand and overall bed expansions of 200% or more can be achieved (Heinen et al., 1996; Tsukuda et al., 1997; Nam et al., 2000; Summerfelt et al., 2004b). In addition, biosolids retention is especially high within FSBs using fine sands, up to 35,000 mg/L of TVS have been measured within the FSB (Tsukuda et al., 1997), because this type of FSB is operating at a relatively low superficial water velocity that does not tend to shear off and washout biofilm as would be the case with a larger sand. Portions of biofilm that are sloughed from the sand are flushed toward the top of the FSB. With fine sand FSBs, however, the water velocity through the bed is insufficient to lift the larger biofilm particles clear of the bed interface and the bed grows deeper with time (Tsukuda et al., 1997; Nam et al., 2000). When necessary, excess biosolids in fine sand FSBs must be siphoned from the top of the bed to prevent the top of the bed from reaching the outlet of the FSB. In contrast, when a larger sand (e.g., $D_{10} > 0.4$ mm) is used within a FSB, the superficial water velocity required to maintain bed expansion is possibly 2–4 times greater than the water velocity required for the fine sand FSB (Tsukuda et al., 1997). Higher water velocities and larger sand grains both increase biofilm shear and work to maintain extremely thin biofilm coatings on these larger sands, with correspondingly lower TVS concentrations (i.e., 1600–3000 mg/L) measured in these FSBs (Tsukuda et al., 1997). Biosolids retention in FSBs with larger sands is reduced because the higher water velocity in these vessels tends to carry most of the sloughed biosolids out the top of the biofilter (Tsukuda et al., 1997).

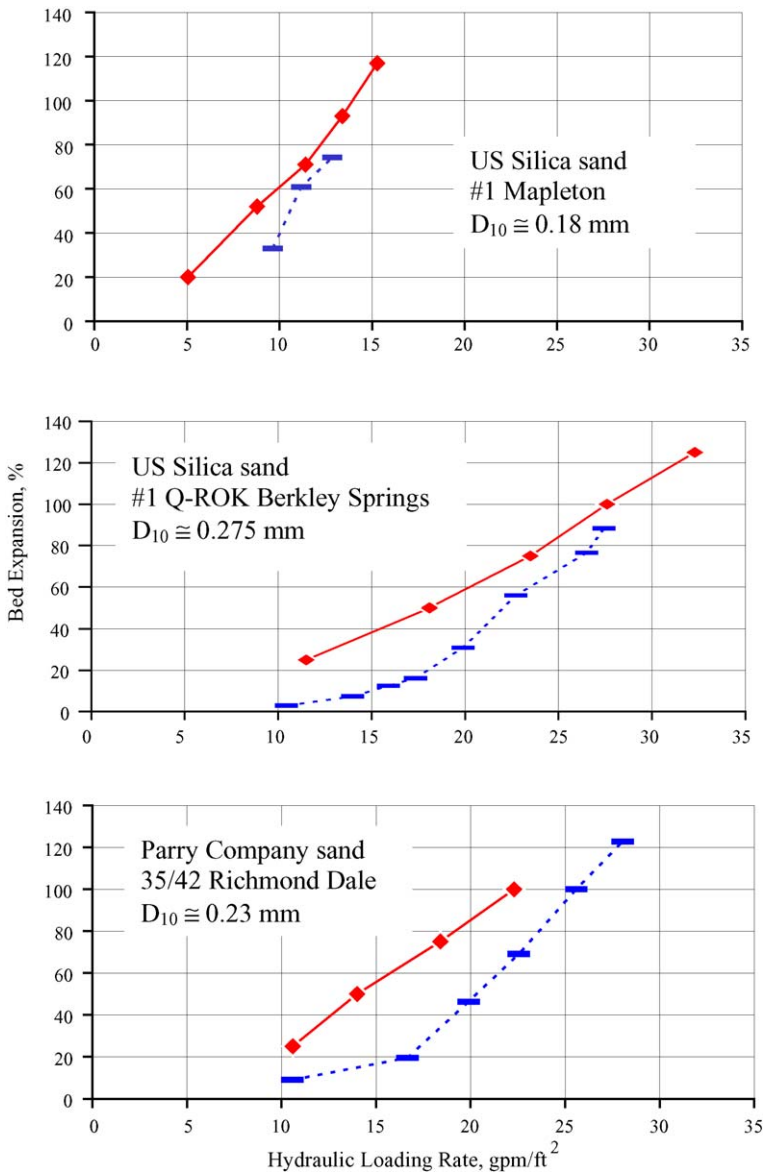

Fig. 6. Comparison of three sands in expansion tests in a 2.7 m diameter fluidized-sand CycloBio® biofilter (▬) vs. tests within a 10 cm test column (◆) (from Summerfelt et al., 2004b).

The FSB vertically stratifies as the largest sand fractions migrate towards the bottom of the bed and the finest sand fractions migrate towards the top of the bed, and because the controlling mechanisms in biofilm growth are also vertically stratified (Summerfelt and Cleasby, 1996; Nam et al., 2000). In the lower portion of the FSB, biofilm encounters the highest substrate loading, the largest sand size, the least bed expansion, and the strongest particle–particle/particle–wall interactions due to increased turbulence around fluid injection sites and due to larger grain sizes and less expansion (Summerfelt and Cleasby, 1996). The upper portion of the FSB has the lowest substrate loading, the smallest grain size, the greatest

bed expansion, and the weakest particle–particle/particle–wall interactions. The resulting vertical stratification, at least in fine-sand biofilters used in recirculating aquaculture systems, is controlled by physical mechanisms at the bottom of the bed and growth mechanisms in the upper portion of the bed (Summerfelt and Cleasby, 1996). The bottom portion of the FSB consists of relatively larger sand grains that are coated with biofilms so thin that they are not visible to the naked eye, whereas, the upper portion of the FSB consists of finer sand with thick biofilm and conglomerates consisting of large biosolid particles that may or may not contain sand grains (Summerfelt and Cleasby, 1996; Nam et al., 2000). The middle portion of the FSB can consists of both biofilm types, depending upon conditions. In fluidized-bed biofilters used in aquaculture, a sharp density boundary has often been observed between the two distinct layers, i.e., between the scoured sand layer and the biofilm-coated sand layer (Summerfelt and Cleasby, 1996; Nam et al., 2000). At light loads in larval systems, no sludge layer is obtained, even with very fine media (Weaver, 2005).

4. Fluidized-sand biofilter design and performance criteria

FSBs used in recirculating aquaculture systems must be sized to remove 100% of the total ammonia-nitrogen (TAN) produced daily. A mass balance that accounts for TAN production and removal should be used to determine the rate that water is exchanged through the biofilter in order to maintain a TAN concentration within the fish culture tank(s) that is below a specified limit (Timmons et al., 2002; Summerfelt and Vinci, 2004). In most instances, the mass balance indicates that the biofilter must treat anywhere from 50 to 100% of the total flow passing through the fish culture tank. The recirculating water that does not have to be treated by the biofilter is typically required for transporting additional dissolved oxygen or to provide more dissolved carbon dioxide removal.

The size of the biofilter (e.g., cross-sectional area and bed depth) and size of the sand selected sets the potential treatment capacity of the biofilter. Selection of the sand and desired bed expansion also sets v_0. Once the biofilter flow rate (Q_{biof}, L/min) has been identified and a v_0 assumed for a given sand, the cross-sectional area (A_b) requirements for the fluidized bed can be calculated:

$$A_b = \frac{Q\,(\mathrm{L/min})}{v_0\,(\mathrm{cm/s})}\,\frac{1000\,(\mathrm{cm^3})}{1\,(\mathrm{L})}\,\frac{1\,(\mathrm{min})}{60\,(\mathrm{s})}\,\frac{1\,(\mathrm{m^2})}{100\,(\mathrm{cm})^2} \tag{12}$$

If necessary, the design can be modified by adjusting tank diameter and sand diameter to provide a tank of convenient size, to allow the use of a graded sand which is available locally, or to increase the potential treatment capacity of the filter (Summerfelt, 1996).

The static sand placed into a FSB is generally designed to be 1–2.5 m deep (3–8 ft), in part due to practical considerations such as overall vessel height limitations, vessel geometry restrictions, total head-loss limits, and bed oxygen demand. Overall expanded bed depth can range from under 2 m to over 5 m, depending upon the situation (Tsukuda et al., 1997; Summerfelt et al., 2004b). However, the sand depth must provide a total bed volume (typically considered as total expanded bed) or a total available surface area sufficient to ensure that 100% of the TAN produced daily can be readily assimilated in the FSB.

As summarized by Timmons et al. (2002) and Summerfelt and Vinci (2004), the most important factors in the design of a biofilter are (1) the mass of TAN that it removes per day, i.e., the product of the flow rate across the biofilter and the change in concentration of ammonia across the biofilter; (2) the TAN removal efficiency (f_{rem}) of the biofilter. The mass of TAN removed per day can often be increased as the hydraulic loading rate is increased across a biofilter. However, increased hydraulic loading rate (i.e., v_0) across FSBs can decrease the TAN removal efficiency as the water retention time is shortened and the mass load of TAN is increased (Tsukuda et al., 1997).

The concentration of TAN discharged from a culture tank (TAN_{out}, mg/L) is controlled by the f_{rem} of TAN across the biofilter, the average daily rate that TAN is produced, i.e., r_{TAN} (kg waste per day), the fraction of water flow that is reused, i.e., R (unitless), and the flow rate of water recirculated through the biofilter, i.e., Q_{biof} (L/min) according to the following

equation, which was first developed by Liao and Mayo (1972):

$$\mathrm{TAN_{out}} = \left\{ \frac{1}{1 - R + (R f_{\mathrm{rem}})} \right\} \times \left\{ \frac{r_{\mathrm{TAN}}}{Q_{\mathrm{biof}}} \frac{10^6\,(\mathrm{mg})}{1\,(\mathrm{kg})} \frac{1\,(\mathrm{day})}{1440\,(\mathrm{min})} \right\} \quad (13)$$

This equation was derived from mass balances that assume that no waste accumulation can occur in a culture tank, that the make-up water contains no TAN, and that the recirculating system is operating under steady-state conditions, i.e., water flow rates, waste production rates, and unit process treatment efficiencies are relatively constant (Timmons et al., 2002).

Most recirculating aquaculture systems operating in temperate climates reuse high fractions of their flow (to conserve heated water) and generally operate with only 5–100% of the total system water volume exchanged daily, equivalent to a fraction of water flow reused $R \geq$ about 0.96 (Timmons et al., 2002; Summerfelt et al., 2004a). In such recirculating systems, waste accumulation depends mainly upon the f_{rem} across the water treatment units and Eq. (14) simples to

$$\mathrm{TAN_{out}} \cong \left\{ \frac{1}{f_{\mathrm{rem}}} \right\} \left\{ \frac{r_{\mathrm{TAN}}}{Q_{\mathrm{biof}}} \frac{10^6\,(\mathrm{mg})}{1\,(\mathrm{kg})} \frac{1\,(\mathrm{day})}{1440\,(\mathrm{min})} \right\} \quad (14)$$

Eq. (13) or (14) should be used to estimate water flows that are required to achieve the desired $\mathrm{TAN_{out}}$, when an accurate estimate of the biofilter f_{rem} is available. The biofilter treatment efficiency that is used during these design calculations should be based upon measurements taken on biofilter TAN inlet and outlet concentrations that were collected under conditions that would be similar to those in the design. The following section of this paper will report f_{rem} across FSBs that range from less than 0.1 to greater than 0.9, depending upon the sand size selected, although large number of studies and commercial applications indicate that removal efficiency across fine sand FSBs will consistently achieve TAN removal efficiencies of >80–90%. Other biofilter types have their own specific f_{rem}, which will depend upon their design and operating conditions, but f_{rem} typically achieved within other commercial-scale biofilter types typically range from 0.1 to 0.5 (Nijhof, 1995; Greiner and Timmons, 1998; Brazil, 2005). When the TAN concentration in the fish culture tank is held constant, a low f_{rem} results in higher water flow requirements that, even at relatively low head, can produce rather high energy requirements to move sufficient water to meet the TAN concentration limit. Overestimates of the biofilter f_{rem} would result in the design of a water recirculating system that could not maintain TAN concentrations within the culture tank within the limits defined in the design.

4.1. Nitrification rate and ammonia removal efficiency

The total surface area available for microbial attachment is the principle design parameter used to define the mass of TAN that a biofilter can remove daily. However, FSBs present an interesting dilemma regarding the effective use of surface area, as typical filter sands used in FSBs provide specific surface areas of anywhere from 4000 to 20,000 $\mathrm{m^2/m^3}$. The specific surface area of a loosely-packed bed of static sand (S_{b}) is relatively large because specific surface area is inversely proportional to the mean diameter of the sand (D_{50}) as described by the equation:

$$S_{\mathrm{b}} = \frac{6(1-\varepsilon)}{\Psi D_{50}} \quad (15)$$

where ε of a loose packed static bed can be assumed to be 0.45, Ψ can be assumed to be 0.75, and D_{50} can be estimated using the following equation (J. Cleasby, Iowa State University, Ames, IA, pers. commun.):

$$D_{50} = D_{10} \times 10^{0.83 \log_{10}(\mathrm{UC})} \quad (16)$$

In the case of FSBs, it has not been clear whether the nitrification rate on sand is more accurately based on the total expanded bed volume or on the total sand surface area. The specific surface area of a sand bed is so high that the thickness of the biofilm coating the sand and the presence of bio-floc particles changes the relationship between TAN treatment capacity and surface area. Therefore, the total volume of the expanded bed will likely provide a better reflection of a FSBs treatment capacity than the total surface area within the bed.

Sand size controls the bed's specific surface area (Eq. (15)), the water velocity required to achieve a

Table 4
Average concentrations (±S.E.) of dissolved oxygen, total ammonia-nitrogen, and nitrite in the test column influent and effluents reported by Tsukuda et al. (1997)

Parameter	Influent concentration (mg/L)	Effluent concentration (mg/L) at effective sand size			
		0.23 mm	0.45 mm	0.60 mm	0.80 mm
Dissolved oxygen	10.05 ± 0.16	5.69 ± 0.19	9.08 ± 0.24	9.54 ± 0.21	9.61 ± 0.15
Total ammonia-nitrogen	0.62 ± 0.04	0.07 ± 0.02	0.55 ± 0.04	0.57 ± 0.04	0.57 ± 0.05
Nitrite	0.038 ± 0.002	0.067 ± 0.005	0.061 ± 0.004	0.051 ± 0.004	0.045 ± 0.006

given expansion (Eqs. (7), (9) and (10)), the hydraulic retention time through the biofilter, the shear forces between biofilm-coated sand particles, and the ammonia, oxygen, and organic matter loading rates, which are the product of the biofilter inlet concentration times water flow rate. Therefore, in fluidized-sand biofilters, sand size will also have an effect on the rate and efficiency of ammonia, nitrite, and oxygen removal, as well as the biofilm thickness and accumulation of biosolids in the bed. The efficiency of nitrification per unit surface area is dependent upon the accessibility of the surface to the substrate, the substrate concentration and loading, the mass transfer rate into and out of the biofilm, the growth phase of the biofilm (lag, log, stationary, and death phases), and by the competition with heterotrophic microbes for space and oxygen (Chang et al., 1991; Manem and Rittman, 1992). Efficient use of the sand surface area is provided in fluidized beds by the suspension and rolling of the media grains such that all portions are exposed to the solution. Mass transfer efficiency is increased at the biofilm surface on the particles within the fluidized bed because the high velocities and turbulence required for bed expansion decreases the thickness of the stagnant boundary layer surrounding the biofilm. Biofilm age can be managed by either introducing clean sand while removing aged biofilms from the top of the FSB, or, by selecting a sand diameter that maintains a relatively thin steady-state biofilm, one with no net change in growth or decay. Plug flow of water through the FSB also serves to increase TAN removal efficiency in comparison to completely mixed stirred tank reactors, as discussed by Watten and Sibrell (2005).

Several studies of FSB nitrification in salmonid recirculating systems and in warm water recirculating system are discussed below.

Pilot-scale tests evaluating four sand sizes, Tsukuda et al. (1997). Tsukuda et al. (1997) reports on tests of pilot-scale fluidized-sand biofilters that were operated in parallel with an established fluidized bed sand biofilter in a cold-water recirculating system used to produce food-size rainbow trout. An 8-week trial involving twelve 10 cm diameter columns was conducted to determine the nitrification rate and efficiency of four different sand sizes, i.e., D_{10} = 0.23, 0.45, 0.60 and 0.80 mm, that were each replicated three times and that were operated at constant velocities, i.e., 0.82, 1.8, 2.8, and 3.8 cm/s, respectively, for each sand size. Before this study began, the 12 FSBs were given 15 weeks to develop a nitrifying biofilm. Change in TAN, nitrite-nitrogen, and dissolved oxygen concentrations were measured across each column during the study (Table 4). The average removal efficiency and average removal rate for each of these parameters are reported in Tables 5 and 6. Effluent TAN concentrations leaving the FSBs containing the finest sand were only 0.06 mg/L,

Table 5
Average removal efficiencies (±S.E.) of dissolved oxygen and total ammonia-nitrogen across the four different sand sizes as reported by Tsukuda et al. (1997)

Parameter	Removal efficiency (%) at effective sand size			
	0.23 mm	0.45 mm	0.60 mm	0.80 mm
Dissolved oxygen	43 ± 1	10 ± 1	5 ± 1	4 ± 1
Total ammonia-nitrogen	89 ± 2	11 ± 2	8 ± 2	8 ± 3

Table 6
Mean ammonia removal rates (±S.E.) across the four different sand sizes as reported by Tsukuda et al. (1997)

Total ammonia-nitrogen removal rates	At effective sand size			
	0.23 mm	0.45 mm	0.60 mm	0.80 mm
g/day	8.0 ± 0.5	2.2 ± 0.3	2.5 ± 0.5	3.2 ± 1.2
kg/m^3 biofilm expanded bed per day	0.41 ± 0.03	0.19 ± 0.03	0.31 ± 0.06	0.39 ± 0.15
kg/m^3 clean static bed per day	1.5 ± 0.09	0.48 ± 0.07	0.45 ± 0.09	0.56 ± 0.21
g/m^2 clean sand per day	0.13 ± 0.01	0.06 ± 0.01	0.08 ± 0.02	0.13 ± 0.05

whereas, effluent TAN concentrations leaving the FSBs containing the three largest sands were from 0.55 to 0.57 mg/L (Table 4). This data clearly indicated that the smallest sand size ($D_{10} \approx 0.23$ mm) removed the largest percentage of TAN each pass through the FSB, i.e., 89% removal, whereas the three larger sands only removed 8–11% of the TAN each pass (Table 5). However, this data did not clearly indicate whether-or-not TAN removal rates were more appropriately expressed in expanded volume or available surface area (Table 6). The TAN removal rate expressed per unit expanded bed volume ranged from 0.19 to 0.41 kg ammonia/m^3/day across all four sand sizes (Table 6).

Full-scale study on nitrification in a FSB operated with or without an internal biofilm stripping mechanism (unpublished). Biofilm stripping devices have been used to shear thick biofilm from sand since the early 1970s in commercial wastewater treatment units (Sutton and Mishra, 1991). However, control of biofilter bed expansion in fine-sand FSBs found in recirculating aquaculture systems is typically achieved by simply siphoning off excess bed growth when it comes within 0.3–0.6 m of the vessel outlet. In a 310 day unpublished research study conducted at TCFFI, S. Summerfelt, M. Durant, and D. Bullock evaluated a mechanism for stripping thickening biofilms within a FSB to control bed growth and reduce the size of biosolids contained within the bed. A horizontal pipe manifold type FSB was tested that was 1.52 m diameter by 2.44 m tall. The FSB was operated in a recirculating salmonid production system that was previously described by Heinen et al. (1996). During this study, the estimated trout biomass in the recirculating system averaged 814 kg (ranging from 684 to 981 kg due to stocking and harvesting events) and the mass of feed fed weekly averaged 174 kg. A pump was used to force the biosolid particles that collect near the top of the bed to near the bottom of the bed where the fluid shear was greatest. A small magnetic drive submersible pump (Little Giant) was used to move the relatively larger bio-particles from near the top of the bed to its base, which was in the scoured-sand region of the bed. The magnetic drive submersible pump did not wear-out from sand abrasion during 230 days of use. The ammonia, nitrite, and oxygen concentrations in the biofilter inlet and outlet flow were measured approximately three times weekly. Sand samples were collected weekly from the biofilter at three different depths and these samples were analyzed for size of clean sand and overall diameter of the larger bio-particles (Table 7) – which look similar to large brown cottage cheese curds – contained in the samples using a digital image analysis software package (Mocha®, Jandel Scientific, San Rafael, CA). Data collected during the period before the biofilm stripping mechanism was added to the biofilter was compared to data collected during operation of the biofilm stripping mechanism (Table 7). Results from this study indicate that the FSB was vertically stratified with respect to sand size, bio-particle size, and expansion (Table 7). Results also indicate that the diameter of the larger bio-particles could be reduced by operating the biofilm stripping mechanism (Table 7). Pumping the biosolids from the top of the biofilter bed to the bottom of the bed must have increased the opportunity for the biofilm to shear because of the more intense physical interactions produced by the pump impeller, vessel bottom, and the larger sand grains located in the lower portion of the bottom. The turbulent conditions and water jets in the water injection regions at the bottom of the sand bed were also thought to contribute favorably to biofilm scouring. The combined depth of the sand and biosolids in the biofilter averaged 1.93 ± 0.01 m

Table 7
Diameter (mean ± S.E.) of cleaned sand and of "bio-floc" particles collected from the upper, middle, and lower portions of the FSB

	Mean sand size (mm)	"Bio-floc" diameter (mm)	Bed expansion (%)
Stripper "off"			
Upper bed	0.289 ± 0.004	1.096 ± 0.077	257 ± 18
Middle bed	0.319 ± 0.005	1.706 ± 0.114	203 ± 13
Lower bed	0.420 ± 0.004	None present	59 ± 7
Stripper "on"			
Upper bed	0.305 ± 0.004	0.887 ± 0.044	231 ± 20
Middle bed	0.330 ± 0.003	0.936 ± 0.031	207 ± 11
Lower bed	0.430 ± 0.004	None present	68 ± 4

In addition, approximate bed expansions are reported for samples taken from upper, middle, and lower regions of the biofilter and fluidized in 10.2 cm diameter test columns at a superficial velocity of 0.63 cm/s.

(76 ± 1 in.) and 1.76 ± 0.03 m (69 ± 1 in.), respectively, during the control period and the period when the biofilm stripping mechanism was activated. However, the biofilm stripping mechanism was able to maintain a fairly constant bed depth without the having to siphon biosolids from the top of the bed, which was required when the biofilm stripping mechanism was not in use.

The TAN and nitrite-nitrogen concentrations exiting the FSB biofilter were both low, i.e., TAN was 0.08 and 0.12 mg/L and nitrite-nitrogen was 0.04 and 0.07 mg/L, when operated with or without the biofilm stripping mechanism, respectively (Table 8). In addition, TAN removal efficiency and removal rate were comparable, i.e., removal efficiency of 88 and 82% and removal rate of 164 and 146 g TAN removed per day per cubic meter of expanded bed, when operated with or without the biofilm stripping mechanism, respectively (Table 8).

After completing this study, the authors concluded that, although the biofilm stripping mechanism was effective at controlling bed expansion and did not reduce the performance of the FSB, it was considered undesirable to increase biofilm shearing and washout of fine biosolids from the FSB because this in turn would increase the number of fine solids coming in contact with fish gills. Producing fine solids within a water recirculating system may not be of much concern when the fish species cultured can withstand high levels of suspended solids.

Full-scale study on nitrification in a CycloBio® FSB, Summerfelt et al. (2004b). Nitrification within a 2.74 m (9 ft) diameter × 6.0 m (20 ft) tall CycloBio® FSB in a recirculating salmonid system at TCFFI (described by Summerfelt et al., 2004a) was evaluated during 2 years of operation using a Parry Company 35/42 Richmond Dale silica sand, i.e., $D_{10} \cong 0.23$ mm, and over 8 months of operation using the US Silica

Table 8
Total ammonia-nitrogen (TAN), nitrite-nitrogen, and oxygen biofilter inlet and outlet concentrations, as well as biofilter removal efficiencies and removal rates within a FSB operated with or without a biofilm shearing mechanism

	Biofilter inlet (mg/L)	Biofilter outlet (mg/L)	Removal efficiency (%)	Removal rate (g/day/m^3 of expanded bed)
Stripper "off"				
TAN	0.63 ± 0.02	0.12 ± 0.02	82 ± 2	146 ± 8
Nitrite-nitrogen	0.10 ± 0.02	0.07 ± 0.02	90 ± 2	157 ± 9
Oxygen	10.0 ± 0.2	6.2 ± 0.2	38 ± 2	1070 ± 80
Stripper "on"				
TAN	0.66 ± 0.01	0.08 ± 0.01	88 ± 1	164 ± 5
Nitrite-nitrogen	0.06 ± 0.00	0.04 ± 0.00	94 ± 0	169 ± 5
Oxygen	9.4 ± 0.3	4.5 ± 0.2	50 ± 3	1380 ± 140

Table 9
Nitrification performance using two different sands in a full-scale CycloBio® FSB as reported by Summerfelt et al. (2004b)

	#1 Mapleton sand		35/42 Richmond Dale sand	
	1.1% makeup	6.4% makeup	3.4% makeup	8.4% makeup
Total ammonia-nitrogen				
Biofilter inlet (mg/L)	1.49 ± 0.04	1.18 ± 0.04	1.68 ± 0.02	1.07 ± 0.11
Biofilter outlet (mg/L)	0.22 ± 0.01	0.09 ± 0.01	1.02 ± 0.05	0.38 ± 0.01
Biofilter delta TAN (mg/L)	1.24 ± 0.03	1.09 ± 0.03	0.660 ± 0.066	0.69 ± 0.10
TAN removal efficiency (%)	83.1 ± 0.2	92.2 ± 0.7	39.3 ± 3.5	64.2 ± 2.9
TAN removal rate, g/day/m^3 of expanded bed depth	160	140	170	170
Nitrite-nitrogen				
Biofilter inlet (mg/L)	0.28 ± 0.03	0.06 ± 0.00	0.72 ± 0.02	0.27 ± 0.02
Biofilter outlet (mg/L)	0.25 ± 0.07	0.02 ± 0.00	0.74 ± 0.01	0.31 ± 0.01
Dissolved carbon dioxide				
Biofilter inlet (mg/L)	25 ± 0	20 ± 2	–	–
Biofilter outlet (mg/L)	28.5 ± 2	28 ± 2	–	–
Biofilter delta CO_2 (mg/L)	4 ± 2	8 ± 1	–	–
Dissolved oxygen				
Biofilter inlet (mg/L)	9.4 ± 0.1	10.9 ± 0.4	–	–
Biofilter outlet (mg/L)	2.5 ± 0.0	4.6 ± 0.1	–	–
Biofilter delta O_2 (mg/L)	6.9 ± 0.2	6.4 ± 0.3	–	–
Dissolved organic carbon				
Biofilter outlet (mg/L)	7.4 ± 0.1	2.7	8.1 ± 0.1	4.1 ± 0.7
Makeup flow, % total flow	1.1 ± 0.0	6.4 ± 0.1	3.4 ± 0.1	8.4 ± 0.3
Feed (kg/day)	126.4 ± 3.1	136.7 ± 11.7	143.2 ± 4.6	152.7 ± 0
Flow through biofilter (L/min)	2696 ± 17	2716 ± 6	4497 ± 11.5	4447 ± 0
Biofilter bed depth (m)	5.27 ± 0.01	5.27 ± 0.01	4.37 ± 0.01	4.37 ± 0.01

Company's #1 Mapleton silica sand, i.e., $D_{10} \cong 0.18$ mm (Summerfelt et al., 2004b). In the first nitrification study, the CycloBio® FSB contained the coarser of the two sands (e.g., the 35/42 Richmond Dale sand) and the entire recirculating water flow, approximately 4500–4800 L/min, was pumped to the base and up through the top of CycloBio® fluidized-sand biofilter. In the second nitrification study, the CycloBio® contained the finer of the two sands (e.g., the #1 Mapleton sand) and only 60% of recirculating water flow, approximately 2700 L/min, was pumped through the vessel (Table 9). The remaining 40% of the flow by-passed the CycloBio® and flowed directly to the top of the cascade aeration column. The initial overall 'clean' sand bed expansion was approximately 40% in the first study and approximately 60% in the second study. However, after a biofilm was established, overall bed depth was allowed to grow to 4.37 m (190% expansion) and 5.27 m (216% bed expansion), respectively, for the coarser (35/42 Richmond Dale) sand and the finer (#1 Mapleton) sand. Bed depth was maintained at or below these levels by continuously siphoning biofilm from the top of the bed. The v_0 through the CycloBio® was approximately 1.36 cm/s (20 gpm/ft^2) and 0.77 cm/s (11 gpm/ft^2) for the coarser (35/42 Richmond Dale) sand and the finer (#1 Mapleton) sand, respectively.

With the finer (#1 Mapleton, $D_{10} = 0.18$ mm) sand, the fluidized-sand CycloBio® biofilter maintained >80–90% TAN removal efficiency each pass through the biofilter (Table 9). Typical makeup water flow rates were 4–8% of total recirculating flow and under these conditions TAN removal efficiencies averaged 92.2 ± 0.7% and nitrite-nitrogen concentrations averaged 0.06 ± 0.00 mg/L (Table 9). When makeup water flows were reduced to approximately 1% of the total recirculating flow, dissolved organic carbon concentrations increased to approximately 7.4 ± 0.05 mg/L, the TAN removal efficiency dropped to 83.1 ± 0.2%, and nitrite-nitrogen concentrations rose to 0.28 ± 0.03 mg/L (Table 9). Dissolved oxygen was never limiting within the biofilter, as total dissolved oxygen con-

sumption across the biofilter containing the finer sand averaged 6.4–6.9 mg/L, when it was supporting 126–137 kg/day feed loading on the system (Table 9).

With the coarser (35/42 Richmond Dale, $D_{10} \cong 0.23$ mm) sand, the fluidized-sand CycloBio® biofilter typically maintained TAN removal efficiencies of $64.2 \pm 2.9\%$ and nitrite-nitrogen concentrations of 0.31 ± 0.01 mg/L when supporting a relatively high feed loading rate (152.8 kg/day). When makeup water flows were reduced to approximately 3.4% of the total recirculating flow, dissolved organic carbon concentrations increased to approximately 8.1 ± 0.1 mg/L, the TAN removal efficiency dropped to $39.3 \pm 3.5\%$, and nitrite-nitrogen concentrations rose to 0.74 ± 0.01 mg/L (Table 9).

This data indicates that, as the recirculating system makeup flow was restricted, the resulting accumulation in dissolved organic carbon concentration decreased TAN removal efficiencies and increased the steady state concentrations of TAN and nitrite-nitrogen, especially when the FSB was not operated with the more efficient of the two sand sizes that were evaluated. However, TAN removal rate ranged from 140 to 170 g/day/m^3 of expanded bed depth over all conditions tested (Table 9).

Summary of nitrification results. Data from the two full-scale FSB studies described above (Tables 8 and 9) indicate that TAN removal efficiencies depend upon sand size (Tsukuda et al., 1997; Summerfelt et al., 2004b). These studies indicated that TAN removal efficiencies of >80–90% could be achieved when a fine sand was used (i.e., $v_0 \approx 0.63-0.77$ cm/s), but that TAN removal efficiency declined sharply with larger sand sizes. Data from the two full-scale FSB studies described above (Tables 8 and 9) also indicate that TAN removal rates of 140–170 g/day/m^3 of expanded bed depth have been consistently provided under widely different conditions in full-scale FSB contained in coldwater recirculating systems. TAN removal rates as high as 400 g/day/m^3 of expanded bed depth were achieved in test columns. Thomasson (1991), Monaghan et al. (1996), and Shea et al. (1997) have studied nitrification on larger sands in FSBs found in warmwater systems. In warm water systems, TAN removal rates range from 0.6 to 1.0 kg/day/m^3 expanded bed volume (Timmons and Summerfelt, 1998). The optimum sand size for use in warm-water systems (i.e., at 25–30 °C) appears to be closer to 0.5–0.7 mm, e.g., ranging from a 20 to 40 mesh sand to a 16–30 mesh sand, where these sands are expanded approximately 50% with water velocities (v_0) of 2.0 and 3.2 cm/s, respectively (Timmons and Summerfelt, 1998).

4.2. Carbon dioxide production and dissolved oxygen consumption

Nitrifying bacteria and heterotrophic microorganisms in a FSB will respire and produce a net increase in dissolved carbon dioxide and a net decrease in dissolved oxygen. The production of dissolved carbon dioxide within the biofilter can be estimated from measurements of the concentrations of dissolved oxygen and TAN removed from the water flowing through the biofilter. Approximately 5.9 mg/L of CO_2 is produced and approximately 4.6 mg/L of dissolved oxygen is consumed for every 1 mg/L of TAN consumed across a submerged biofilter (Summerfelt and Sharrer, 2004). In addition, approximately 1.38 mg/L of CO_2 are produced for every 1 mg/L of dissolved oxygen consumed (Summerfelt and Sharrer, 2004). During the Summerfelt and Sharrer (2004) study, the FSB at TCFFI produced 4.1 ± 0.2 mg/L of carbon dioxide while removing 0.51 ± 0.02 mg/L TAN and removing 3.8 ± 0.2 mg/L dissolved oxygen. During the same period the fish produced 6.9 ± 0.4 mg/L of carbon dioxide within this same recirculating flow, so the FSB accounted for approximately 37% of the total carbon dioxide concentration produced within this recirculating salmonid system. Across a more heavily loaded FSB described by Summerfelt et al. (2004b), the dissolved carbon dioxide production has averaged as much as 8 mg/L (Table 9). In addition, dissolved oxygen concentrations exiting the FSBs are relatively low, ranging from 2.5 to 6.2 mg/L (Tables 4, 8 and 9) within the studies summarized above. Approximately 60% of the dissolved oxygen consumed in the FSB operated in a coldwater recirculating system goes towards nitrification (Summerfelt and Sharrer, 2004). Therefore, for every 1 mg/L of TAN removed across the FSB, approximately 7.7 mg/L (=4.6 mg/L DO/0.6) of dissolved oxygen will be consumed, which assumes that 60% of the dissolved oxygen consumed went towards TAN removal. Consequently, oxygen limitations within FSBs can become a problem when the desired removal of TAN is high, i.e., greater than 0.8–

1.2 mg/L across the FSB, depending upon concentration of dissolved oxygen entering the FSB that was assumed to be the saturation concentration in cold and warm water applications, respectively. According to more traditional wastewater treatment biofilter technologies discussed by Zhu and Chen (2002), dissolved oxygen will begin to limit TAN removal in a submerged biofilter when the ratio of dissolved oxygen to TAN concentration becomes less than 1.5–2.0. Therefore, if the TAN concentration exiting the FSB was 1.0 mg/L, then at least 1.5–2.0 mg/L of dissolved oxygen would have to be present to prevent oxygen from limiting nitrification. In the fine sand FSB applications described above, TAN outlet concentrations were less than 0.3 mg/L, so dissolved oxygen concentration would not be limiting until dissolved oxygen concentrations approached 0.6 mg/L.

To counter the dissolved carbon dioxide production and dissolved oxygen consumption across the FSB – and also across the fish culture tank(s) within this recirculating system – a forced-ventilated cascade aeration column is typically placed immediately after the FSB to reduce dissolved carbon dioxide concentrations and increase dissolved oxygen concentrations to near saturation (Summerfelt et al., 2003; Summerfelt and Sharrer, 2004).

5. Fluidized-sand biofilter operation and management practices

5.1. Managing biofilm growth

Biological growth occurs within FSBs, which results in a growing bed that will probably not reach equilibrium before some form of biofilm management must be instituted to avoid washout of lightened biofilm-coated sand (Tsukuda et al., 1997). A disengagement zone between the interface at the top of the expanded bed and the FSB outlet of at least 0.3–1.0 m is necessary to reduce biosolids washout through the FSB outlet. Bio-bed growth is especially common in fine-sand FSBs (i.e., with a D_{10} less than about 0.3 mm), because these biofilters operate at a v_0 that is insufficient to lift the larger biofilm particles clear of the vessel and the bed grows deeper with time (Bullock et al., 1993; Heinen et al., 1996; Summerfelt and Cleasby, 1996; Tsukuda et al., 1997; Timmons and Summerfelt, 1998; Nam et al., 2000; Summerfelt et al., 2004b). When D_{10} exceeds 0.6 mm, biosolids do not accumulate within the expanded sand bed, but detached biofilm particles can sometimes collect in a distinct layer above the expanded sand layer (Tsukuda et al., 1997; Timmons and Summerfelt, 1998).

The expanded bed of biofilm coated sand is fluid, therefore a siphon withdrawing flow and biosolids from one point in the biofilter can remove all fluidized biosolids at depths above this level (for all sand sizes). Thus, bed expansion can be managed by removing biofilm-coated sand or by stripping the biofilm off the sand by increasing the physical shear forces. Siphoning the biosolids from the top of the expanded bed is a relatively simple and frequently used technique to manage bed expansion (Bullock et al., 1993; Heinen et al., 1996; Summerfelt and Cleasby, 1996; Tsukuda et al., 1997; Timmons and Summerfelt, 1998; Summerfelt et al., 2004b). Siphoning the biosolids layer that collects above an expanded bed of relatively large sand (i.e., with a D_{10} of 0.6 mm or larger) is especially simple, because the expansion depth of these sands remains fairly constant and the biosolids can be removed relatively free from sand (Tsukuda et al., 1997; Timmons and Summerfelt, 1998). However, when biosolids are siphoned from beds containing a finer sand, then some sand will be lost when the biosolids are removed. With finer sands, the sand lost during biosolids removal must be replaced within typically 1–2 years. Yet, the cost of sand replacement is relatively low. For example, roughly 50% of the fine-sand in a large-scale CycloBio® FSBs at TCFFI was missing after approximately 2 years of operation. Replacement of this sand would cost $ 500–750 in this biofilter, which was sized to treat the TAN produced by feeding 200 kg daily. However, to prevent the fines contained in the new sand from contacting fish, ideally new sand would only be installed in a recirculating system that does not contain fish or the new sand should be pre-flushed to remove the fines.

Researchers at TCFFI have also investigated controlled biofilm thickness by shearing the biofilm in-vessel using a pump to transport the flocculant particles from the top of the biofilter to the bottom of the bed, where shear forces are greatest. The biofilm stripping system effectively maintained bed

expansion at a fixed level and reduced biofilm thickness without trading-out sand (unpublished data). However, it was concluded that increasing biofilm shearing and washout of fine biosolids from the FSB was undesirable, because this in turn would increase the number of fine solids coming in contact with fish gills.

5.2. Managing flow and avoiding bubbles

A FSB must be operated within a fairly narrow water flow range, i.e., within about ±10–30% of its design flow, in order to maintain proper bed expansion. In addition, water flow through a FSB cannot cease for more than approximately 6–24 h, depending upon conditions, in order to prevent anaerobic condition from occurring that could cause a significant loss in the nitrification capacity of the FSB. When flow is resumed after the FSB has been down for more than 12 h, then the water that is initially flushed can contain elevated concentrations of TAN and suspended solids. Therefore, it is a good management practice to directly discharge the flow of water that was initially flushed through the FSB or let the water recycle while by-passing all of the fish culture tanks – assuming that the recirculating system design allows for this option. Bubbles must also be prevented from entering the FSB, which requires preventing bubbles from entering through leaky pipe fittings or through vortexing or bubble entrainment in the pump sump. Bubbles can create serious problems in FSBs, as they float out sand and biosolids.

5.3. Determining effectiveness of bed expansion

Upon first expansion of the FSB, and then again as often as once a month or as infrequently as biannually, the effectiveness of sand bed expansion should be determined by probing the base of the filter with a pole to establish the depths and locations of sand piles, if any are present. Determining whether the sand bed is uniformly expanded, or not, is necessary to trouble shoot the FSB and determine if the distribution manifold is becoming plugged. If sand mounds taller than about 0.3 m are detected, then it may be necessary to flush debris from the flow distribution manifold.

Depth of the scoured-sand layer should also be determined as an indicator of the total sand available within the bed.

5.4. Mechanisms to unplug the flow distribution manifold

Cleanout of the flow distribution manifold is rarely required. However, cleanout of the flow distribution manifold is necessary in the rare event when the manifold becomes plugged with sand or other debris (Summerfelt et al., 1996), which is most likely to occur if the backflow prevention device is by-passed or malfunctions. At least three of the five types of the FSBs described above (Fig. 1) provide cleanout mechanisms to unplug the flow distribution manifold, i.e., the vertical probe FSB, the horizontal pipe manifold FSB, and the CycloBio® FSB. These three cleanout mechanisms have all been evaluated at TCFFI over the past decade. As an example, a blind flange covering an access port into the annular space of a CycloBio® FSB can be removed[3] to allow a short burst of pumped water to flush sand from that region of the annular space. Then, after the access port has been resealed with the blind flange, the CycloBio® FSB has been found to re-fluidize and clear the remaining sand from the annular chamber (TCFFI, unpublished data). As another example, the lateral pipes in a horizontal pipe manifold can be readily flushed of any plugging debris (Summerfelt et al., 1996) by flushing water down the pipe after the screw caps are removed from the overhead tees at the end of each plugged lateral (Fig. 1). More pressure can be applied to individual laterals by isolating them with valves and applying the entire flow to the obstructions. In addition, a hose supplying pressurized water can be inserted through a clean-out port at the top of each injection pipe (Fig. 1) to backwash any sand or debris from the vertical pipe.

Acknowledgements

This work was supported by the United States Department of Agriculture, Agricultural Research Service, most recently under grant agreement number

[3] Note that the blind flange over the access port into the annular chamber must not be removed until after water inside the vessel has been removed.

59-1930-1-130. I thank Susan Glenn, Thomas Waldrop, Mark Sharrer, John Davidson, Christine Marshall, Daniel Bullock, Graham Bullock, Scott Tsukuda, and Martin Durant for their assistance with the biofilter research. The experimental protocol and methods used in TCFFI biofilter studies were in compliance with Animal Welfare Act (9CFR) requirements and are approved by the Freshwater Institute Institutional Animal Care and Use Committee.

References

American Society for Testing and Materials (ASTM), 1985. Annual Book of ASTM Standards, vol. 04.02, Concrete and Mineral Aggregates ASTM, Philadelphia, PA.

American Water Works Association (AWWA), 1971. Water Quality and Treatment, 3rd ed. McGraw-Hill, New York, NY.

American Water Works Association (AWWA), 1990. Water Treatment Plant Design, 2nd ed. McGraw-Hill, New York, NY.

American Water Works Association (AWWA), 2004. Filter Media – Sand. AWWA Sourcebook AWWA, Denver, CO, p. 151.

Brazil, B.L., 2005. Performance and operation of a rotating biological contactor in a tilapia recirculating aquaculture system. Aquacult. Eng. 34 (3), 261–274.

Bullock, G., Hankins, J., Heinen, J., Starlipper, C., Teska, J., 1993. Quantitative and qualitative bacteriological studies on a fluidized sand biofilter used in a semi-closed trout culture system. Biological Report 17 U.S. Fish and Wildlife Service, Washington, D.C., 15 pp.

Chang, H.T., Rittman, B.E., Amar, D., Heim, R., Ehlinger, O., Lesty, Y., 1991. Biofilm detachment mechanisms in a liquid-fluidized bed. Biotech. Bioeng. 38, 499–506.

Cleasby, J.L., 1990. Filtration. In: Pontius, F.W. (Ed.), Water Quality and Treatment. 4th ed. American Water Works Association/ McGraw-Hill, New York, pp. 455–560.

Cooper, P.F., Atkinson, B., 1981. Biological Fluidized Bed Treatment of Water and Wastewater. Water Research Centre Ellis-Horwood, Chichester, UK.

Denn, M.M., 1980. Process Fluid Mechanics. Prentice-Hall, Englewood Cliffs, NJ.

Dharmarajah, A.H., Cleasby, J.L., 1986. Predicting the expansion of filter media. J. Am. Water Works Assoc. 78 (12), 66–76.

Ergun, S., 1952. Fluid flow through packed columns. Chem. Eng. Prog. 48 (2), 89.

Fan, K.-S., 1981. Sphericity and fluidization of granular filter media. Master's Thesis, Iowa State University, Ames, IA.

Forsythe, A., Hosler, K.C., 2002. Experiences in constructing and operating cold water recirculating aquaculture facilities for salmon smolt production. In: Rakestraw, T.T., Douglas, L.S., Flick, G.J. (Eds.), Proceedings of the Fourth International Conference on Recirculating Aquaculture, Virginia Polytechnic Institute and State University, Roanoke, VA, pp. 325–334.

Goldman, J.N., Rosenau, J.R., 2000. Reissue of US Patent 5,330,652 (RE36,660). Fluidized bed reactor and distribution system. United States Patent and Trademark Office, Alexandria, Virginia.

Geldart, D., 1990. Estimation of the basic particle properties for use in fluid-particle process calculations. Powder Technol. 60, 1–13.

Greiner, A.D., Timmons, M.B., 1998. Evaluation of the nitrification rates of microbead and trickling filters in an intensive recirculating tilapia production facility. Aquacult. Eng. 18, 189–200.

Heinen, J.M., Hankins, J.A., Weber, A.L., Watten, B.J., 1996. A semi-closed recirculating water system for high density culture of rainbow trout. Prog. Fish Culturist 58, 11–22.

Holder, J., 2002. Retrofits of flow through to reuse/recirculation technology. In: Rakestraw, T.T., Douglas, L.S., Flick, G.J. (Eds.), Proceedings of the Fourth International Conference on Recirculating Aquaculture, Virginia Polytechnic Institute and State University, Roanoke, VA, pp. 335–345.

Jewell, W.J., 1990. Fundamentals and advances in expanded bed reactors for wastewater treatment. In: Tyagi, R.D., Vembu, K. (Eds.), Wastewater Treatment by Immobilized Cells. CRC Press, Boca Raton, FL, pp. 223–252.

Liao, P.B., Mayo, R.D., 1972. Salmonid hatchery water reuse systems. Aquaculture 1, 317–335.

Malone, R.F., Burden, D.G., 1988. Design of Recirculating Soft Crawfish Shedding Systems. Louisiana Sea Grant College Program, Center for Wetland Resources, Louisiana State University, Baton Rouge, LA.

Manem, J.A., Rittman, B.E., 1992. The effects of fluctuations in biodegradable organic matter on nitrification filters. J. Am. Water Works Assoc. 84 (4), 147–151.

Monaghan, T.J., Delos Reyes, A.A., Jeansonne, T.M., Malone, R.F., 1996. Effects of media size on nitrification in fluidized sand filters. In: Aquaculture America'96 Book of Abstracts, World Aquaculture Society, Baton Rouge, LA, p. 110.

Montagne, M., 2004. The evolution of two warm water recirculating hatcheries used for propogation of endangered species in the upper Colorado River Drainage System. In: Rakestraw, T.T., Douglas, L.S., Correa, A., Flick, G.J. (Eds.), Proceedings of the Fifth International Conference on Recirculating Aquaculture, Virginia Polytechnic Institute and State University, Roanoke, VA, pp. 273–279.

Montgomery, J.M., Consulting Engineers, Inc., 1985. Water Treatment Principles and Design. John Wiley and Sons, New York.

Nam, T.K., Timmons, M.B., Montemagno, C.D., Tsukuda, S.M., 2000. Biofilm characteristics as affected by sand size and location in fluidized bed vessels. Aquacult. Eng. 22, 213–224.

Nijhof, M., 1995. Bacterial stratification and hydraulic loading effects in a plug-flow model for nitrifying trickling filters applied in recirculating fish culture systems. Aquaculture 134, 49–64.

Shea, G.O., Timmons, M.B., Summerfelt, S.T., Tsukuda, S., 1997. Characterization of fluidized sand beds for warm water systems. In: World Aquaculture'97 Book of Abstracts, World Aquaculture Society, Baton Rouge, LA, p. 421.

Shieh, W.K., Sutton, P.M., Kos, P., 1981. Predicting reactor biomass concentration in a fluidized-bed system. J. Water Pollut. Control Federation 53, 1574–1584.

Summerfelt, S.T., 1996. Engineering design of a water reuse system. In: Summerfelt, R.C. (Ed.), Walleye Culture Manual, NRAC

Culture Series 101. Central Regional Aquaculture Center Publication Center, Iowa State University, Ames, IA, pp. 277–309.

Summerfelt, S.T., Cleasby, J.L., 1996. A review of hydraulics in fluidized-bed biological filters. Trans. Am. Soc. Agric. Eng. 39 (3), 1161–1173.

Summerfelt, S.T., Sharrer, M.J., 2004. Design implication of biofilter carbon dioxide production within recirculating salmonid culture systems. Aquacult. Eng. 32, 171–182.

Summerfelt, S.T., Vinci, B.J., 2004. Avoiding water quality failures. Part 2. Recirculating systems. World Aquacult. 35 (4) 9–11, 71.

Summerfelt, S.T., Wade, E.M., 1998. Fluidized-sand biofilters installed at two farms. Recirc Today 1 (1), 18–21.

Summerfelt, S.T., Hankins, J.A., Durant, M.D., Goldman, J.N., 1996. Removing obstructions: modified pipe-lateral flow distribution mechanism reduces backflow in fluidized-sand biofilters. Water Environ. Technol. 8 (11), 39–49.

Summerfelt, S.T., Bebak-Williams, J., Tsukuda, S., 2001. Controlled systems: water reuse and recirculation. In: Wedemeyer, G. (Ed.), Fish Hatchery Management. 2nd ed. American Fisheries Society, Bethesda, MD, pp. 285–395.

Summerfelt, S.T., Davidson, J.T., Waldrop, T., Vinci, B.J., 2003. Evaluation of full-scale carbon dioxide stripping columns in a coldwater recirculating system. Aquacult. Eng. 28, 155–169.

Summerfelt, S.T., Wilton, G., Roberts, D., Savage, T., Fonkalsrud, K., 2004a. Developments in recirculating systems for arctic char culture in North America. Aquacult. Eng. 30, 31–71.

Summerfelt, S.T., Davidson, J., Helwig, N., 2004b. Evaluation of a full-scale CycloBio fluidized-sand biofilter in a coldwater recirculating system. In: Rakestraw, T.T., Douglas, L.S., Correa, A., Flick, G.J. (Eds.), Proceedings of the Fifth International Conference on Recirculating Aquaculture, Virginia Polytechnic Institute and State University, Roanoke, VA, pp. 227–237.

Sutton, P.M., Mishra, P.N., 1991. Biological fluidized beds for wastewater treatment: a state-of-the-art review. Water Environ. Technol. 3 (8), 52–56.

Thomasson, M.P., 1991. Nitrification in fluidized-bed sand filters for use in recirculating aquaculture systems. Master's Thesis. Louisiana State University, Baton Rouge, LA.

Timmons, M.B., Summerfelt, S.T., 1998. Application of fluidized-sand biofilters. In: Libey, G.S., Timmons, M.B. (Eds.), Proceedings of the Second International Conference on Recirculating Aquaculture, Virginia Polytechnic Institute and State University, Roanoke, VA, pp. 342–354.

Timmons, M.B., Helwig, N., Summerfelt, S.T., 2000. The Cyclone sand biofilter: a new design concept and field evaluation. In: Libey, G.S., Timmons, M.B. (Eds.), Proceedings of the Third International Conference on Recirculating Aquaculture. Virginia Polytechnic Institute and State University, Roanoke, VA, pp. 222–226.

Timmons, M.B., Ebeling, J.M., Wheaton, F.W., Summerfelt, S.T., Vinci, B.J., 2002. Recirculating Aquaculture Systems, 2nd ed. Cayuga Aquaculture Ventures, LLC, Ithaca, NY.

Tsukuda, S.M., Hankins, J.A., Marshall, C.P., Summerfelt, S.T., Bullock, G.L., Sawyer, T.K., 1997. Effects of sand size on fluidized-bed biofilter performance in cold water systems. In: Timmons, M.B., Losordo, T. (Eds.), Advances in Aquacultural Engineering, NRAES-105. Northeast Regional Agricultural Engineering Service, Ithaca, NY, pp. 368–380.

Watten, B.J., Sibrell, P.L., 2005. Comparative performance of fixedfilm biological filters: application of reactor theory. Aquacult. Eng. 34 (3), 198–213.

Weaver, D.E., 1991. Performance of fine sand fluidized bed. In: Proceedings of the Design of High-density Recirculating Aquaculture Systems. Louisiana Sea Grant College Program Publication, Louisiana State University, Baton Rouge, LA, pp. 18–23.

Weaver, D.E., 2005. Design and operations of fine media fluidized bed biofilters for meeting oligotrophic water requirements. Aquacult. Eng. 34 (3), 303–310.

Weber, W.J., 1972. Physicochemical Processes for Water Quality Control. John Wiley and Sons, New York.

Wen, C.Y., Yu, Y.H., 1966. Mechanics of fluidization. In: Chemical Engineering Progress Symposium Series 62, American Institute of Chemical Engineers, New York.

Wilton, S.J., 2002. Design of a 50 T Salmon Smolt Operation. In: Rakestraw, T.T., Douglas, L.S., Flick, G.J. (Eds.), Proceeding of the Fourth International Conference on Recirculating Aquaculture, Virginia Polytechnic Institute and State University, Roanoke, VA, pp. 325–334.

Zhu, S., Chen, S., 2002. The impact of temperature on nitrification rate in fixed film biofilters. Aquacult. Eng. 26, 221–237.